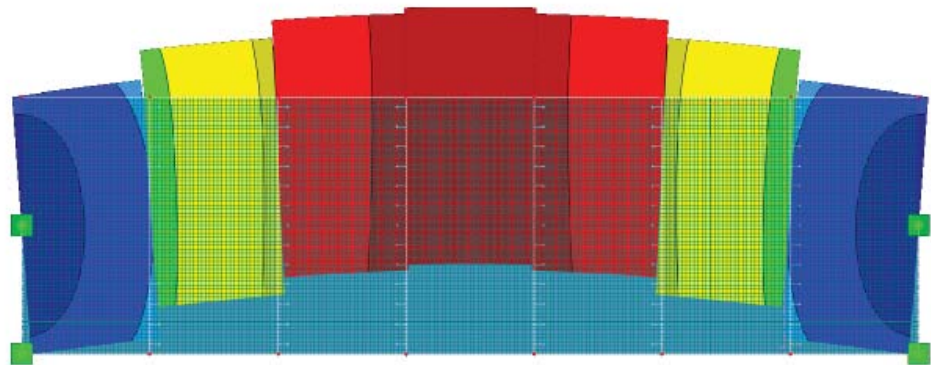




**LUND**  
UNIVERSITY



# **SHEAR STIFFNESS OF CROSS LAMINATED TIMBER DIAPHRAGMS**

**A study of the influence of connection  
and member stiffness**

GUSTAF OLAUSSON

---

Structural  
Mechanics

*Master's Dissertation*

---



DEPARTMENT OF CONSTRUCTION SCIENCES  
DIVISION OF STRUCTURAL MECHANICS

ISRN LUTVDG/TVSM--22/5252--SE (1-67) | ISSN 0281-6679

MASTER'S DISSERTATION

# SHEAR STIFFNESS OF CROSS LAMINATED TIMBER DIAPHRAGMS

A study of the influence of connection  
and member stiffness

GUSTAF OLAUSSON

Supervisor: Dr **HENRIK DANIELSSON**, Division of Structural Mechanics, LTH.

Assistant Supervisor: **EVA FRÜHWALDS HANSSON**, Associate Professor,  
Division of Structural Engineering, LTH.

Examiner: Professor **ERIK SERRANO**, Division of Structural Mechanics, LTH.

Copyright © 2022 Division of Structural Mechanics,  
Faculty of Engineering LTH, Lund University, Sweden.

Printed by V-husets tryckeri LTH, Lund, Sweden, February 2022 *(Pl)*.

**For information, address:**

Division of Structural Mechanics,  
Faculty of Engineering LTH, Lund University, Box 118, SE-221 00 Lund, Sweden.

Homepage: [www.byggmek.lth.se](http://www.byggmek.lth.se)



# Abstract

Since ancient times, buildings have been constructed with the use of timber and during the modern era, new types of timber products have been developed. Today, more constructions, especially residential buildings are being built with timber as the main load-bearing material. By utilizing timber in buildings, the amount of greenhouse gases emitted in production decreases compared to other common materials. The increase in timber buildings is partly due to the implementation of Cross Laminated Timber (CLT) during the late 20th century.

The composition of CLT with crosswise glued boards minimizes the orthotropic behaviour of timber and has a high load-bearing capacity compared to its low self-weight. It is a strong and stiff material useful in diaphragms both in floor- and wall constructions for stabilizing against lateral forces. Due to the crosswise composition, the stiffness varies depending on load direction and fibre orientation with the highest stiffness and strength being in the longitudinal direction of the element. Floor- and wall segments in buildings consisting of CLT-panels are comprised of several panels, connected with each other. The performance of the structure is therefore dependent on the parameters in the connection as well as the element itself.

When utilizing CLT as a floor structure, there are several types of connections which could be applied. For the purpose of stabilizing against lateral forces, *butt joints*, *lap joints* and *spline connections* are the most common used today. They differ in appearance, stiffness and strength but, all of them fasten elements with the use of screws. The connection has to handle forces in between elements due to in-plane bending and shear deformation of the floor diaphragm.

In this work, analytical and numerical modeling and calculations are performed. The shear stiffness for the different types of connections studied is determined, which includes assumptions of inclination angle, screw type, length and diameter of the screw.

Subsequent calculations are made by making use of a finite element structural software, RFEM. The model, containing seven interconnected CLT panels is created in the software with the panels used being modeled according to the plate theory of Mindlin-Reissner. Loads are introduced followed by implementing the laminate add-on in the software, which is crucial as it gives the opportunity to analyze materials composed of layers with different properties. Two behaviours are studied, each with the variation of element stiffness and connection shear stiffness through spring constants. Initially, the displacements are analysed for a simply supported structure. Then, additional supports are modeled while studying the effects of force distribution from the same parameters as the previous study.

Extracting results indicates a higher shear stiffness for equal number of screws is achieved for implementing butt joints with inclined screws in both the vertical and horizontal plane. The same stiffness can be obtained for the other connections, if more screws are installed per metre.

Displacements in the lateral direction of the floor are affected more by the variation of the shear stiffness in the connections compared to the variation of CLT panel stiffness. A decreasing connection stiffness results in an exponentially increasing displacement. However, the results indicate that after a certain limit in stiffness for both parameters, no major variation of displacement takes place. To reduce the magnitude of displacements, a shear stiffness of at least  $4 \text{ N/mm}^2$  is recommended whilst not having a reduction factor for the in-plane shear stiffness of the panel  $k_s$ , which is smaller than 0.3-0.4.

From the results, the distribution of reaction forces depending on the amount of supports is a bit more unclear. However, more supports have a positive effect since it results in distributing the load more evenly with less load on a single support. The parameter contributing to the most even distribution is the shear stiffness in the connection. A higher shear stiffness means less variation of the amount of force that is distributed on the supports. However, more supports tend to have a larger difference between maximum and minimum values when varying the stiffness parameters compared to when varying the reduction factor for the in-plane shear stiffness of the panel  $k_s$ . A high element stiffness in a CLT panel combined with low shear stiffness in the connection between panels, results in more concentrated loads on the middle supports.

Different connections require different amount of screws per metre to reach a sufficient stiffness which in this project was set as  $4 \text{ N/mm}^2$  for the shear stiffness and not reduce the stiffness of the CLT panel by more than 60-70% corresponding to a reduction factor,  $k_s$  for the CLT panel, that is equal or higher than a factor of 0.3-0.4 to obtain small lateral displacement in the floor. The shear stiffness in the connection affects the displacement more than the element stiffness and the distribution of forces for 4 or less supports are more affected by the shear stiffness as the difference is larger when varying the shear stiffness in the connections.

# Sammanfattning

Sedan en lång tid tillbaka har människor uppfört konstruktioner i trä och under modern tid har nya typer av träprodukter utvecklats. Idag byggs det mera, särskilt bostadshus med trä som bärande material. Genom att använda trämaterial i byggnader minskar mängden växthusgaser som släpps ut i produktionen jämfört med andra vanliga material. Ökningen av träbyggnader beror delvis på införandet av korslimmat trä (KL-trä) under slutet av 1900 -talet.

Sammansättningen av KL-trä med korslagda limmade brädor minimerar KL-skivans ortotropi och bidrar till en hög bärförmåga i förhållande till den låga egenvikten. Det är ett starkt och styvt material vilket gör det användbart både i golv- och väggkonstruktioner för stabilisering mot horisontalkrafter. På grund av lagrens olika orientering varierar styvheten beroende på lastriktning och fiberorientering där den högsta styvhet och styrkan uppnås i elementets längdriktning. Golv- och väggkonstruktioner av KL-trä består av flera paneler, som är sammankopplade med varandra. Konstruktionens prestanda är därför beroende av såväl egenskaperna i anslutningen som egenskaperna hos själva elementet.

När man använder KL-trä i golvkonstruktioner finns det flera typer av anslutningar som kan användas mellan elementen. För att stabilisera mot horisontella krafter finns vanligtvis stumfogar, överlappsskarv och skarvar med annat material mellan KL-element. De skiljer sig åt både i utseende och styrka, men för alla varianter ansluts elementen med hjälp av skruvar. Anslutningarna måste hantera krafter som uppstår mellan elementen på grund av skjuvning och böjning i bjälklagsskivans plan.

I arbetet har både analytisk och numerisk modellering och beräkning genomförts. Skjuvstyvheten för varje anslutning som studeras, beräknas med antaganden om vinkel på skruven, skruvtyp, längd och diameter på skruven.

Efterföljande beräkningar görs genom att använda en programvara anpassad för finita element metoden, RFEM. Modellen innehåller sju paneler, anslutna mellan varandra där panelerna modelleras med hänsyn till platteorin enligt Mindlin-Reissner. Belastningar introduceras följt av implementering av RFEMs programtillägg Laminate som är avgörande eftersom det ger möjlighet att analysera material uppbyggda av lager med olika egenskaper. I resultaten studeras sedan förskjutningar och lastfördelning, var och en med variationen av elementstyvhet och skjuvstyvhet i förbanden som parameterstudie. Ursprungligen analyseras förskjutningarna för en enkelt upplagd konstruktion. Sedan modelleras ytterligare stöd när kraftfördelningen i golvkonstruktionen ska studeras med hänsyn till variation av samma parametrar som tidigare.

Resultaten indikerar att en högre skjuvstyvhet uppnås genom att använda stumfogar med vinklade skruvar som vinklas i både det vertikala och horisontella planet. Samma styvhet kan erhållas för de andra anslutningarna om fler skruvar installeras per meter.

Förskjutning i golvets längsriktning påverkas mer av variationen i skjuvstyvhet i an-

slutningarna jämfört med variationen av elementstyvhets. En låg styvhets mellan anslutningarna resulterar i en exponentiellt ökande förskjutning. Resultaten indikerar emellertid att efter en viss styvhetsgräns för båda parametrarna sker ingen kraftig minskning av förskjutningen. För att minimera förskjutningarna rekommenderas en skjuvstyvhets på minst  $4 \text{ N/mm}^2$  mellan anslutningarna samtidigt som elementstyvhets inte reduceras med mer än 30-40% för att säkerställa en låg horisontell förskjutning.

Resultaten visar att fördelningen av reaktionskrafterna beroende på antalet stöd inte är lika klara som när det gäller förskjutningen. Fler stöd medför dock en positiv effekt avseende fördelningen av lasten där fler stöd resulterar i en jämnare fördelning och således inte överbelastar fåtalet stöd. Parametern som bidrar till den jämnaste fördelningen är skjuvstyvhets i anslutningarna. En högre skjuvstyvhets innebär mindre skillnad i reaktionskraft på de olika stöden. Även om detta är giltigt tenderar fler stöd att skapa en större skillnad mellan största och minsta värde när styvhetsparametrarna varierar jämfört med när elementstyvhets varierar med reduktionsfaktorn  $k_s$ . En högre elementstyvhets i KL-skivan kombinerat med en låg skjuvstyvhets i förbanden resulterar i mer koncentrerade laster på stödet i mitten av golvet.

Olika anslutningar kräver ett visst antal skruvar per meter för att uppnå en erforderlig styvhets. På grundval av beräkningarna har en gräns kunnat sättas till ett värde av  $4 \text{ N/mm}^2$  för skjuvstyvhets och inte ha en reduktionsfaktor för elementstyvhets som är lägre än 0.3-0.4 för att därigenom uppnå låga horisontella förskjutningar i golvet. När det kommer till deformationen i längsled är skjuvstyvhets i anslutningarna av större betydelse jämfört med elementstyvhets. Fördelningen av krafter för fyra eller färre stöd påverkas likaså mer av skjuvstyvhets eftersom skillnaden är större när fjäderkonstanten varierar i anslutningarna.

# Acknowledgement

I'm particularly indebted to my supervisors Henrik Danielsson and Eva Frühwald Hansson at LTH who have dedicated time and effort to support my work. Many digital meetings facilitated the development of the initial idea. The content, language and presentation of the project benefited from their genuine interest and insights. Furthermore, our continuous discussions during the spring provided concrete and invaluable feedback on the preliminary result. This project would not have been possible without them.

A special thanks is also due to my examiner Erik Serrano who provided substantial comments on relevant sources in the literature review, theory and calculations. His generous engagement and review guided the development of the project.

In addition, I would like to take this opportunity to thank all the teachers at LTH. They have given other students and me much support and guidance through lectures, seminars and exercises. The knowledge I have obtained during these six years results from this rich and diversified experience.

I would also like to thank my fellow partner in crime during the examination project, Ludwig Winberg, our conversations, motivational talks and jokes during coffee breaks propelled me to progress, building the good habit of working from the campus rather than from the isolation of my home. This time at LTH would undoubtedly have been less fun and colourful without your friendship. There are many more friends, none mentioned but none forgotten, whose acquaintance I have made during coffee breaks in V-café, the freshers-week at LTH, mentorship groups, and trips to the Alps. Thank you to you all!

Finally, I want to express my thanks my family who have given me valuable advice along the way, not the least by reading through this paper.



# Symbols

## Latin letters upper case letters

$A_{gross}$  - Gross area of cross-section  
 $B$  - Diaphragm width  
 $C_{CLT}$  - Stiffness matrix for CLT-diaphragm  
 $C_{ux}$  - Spring constant in the local  $x$ -direction  
 $E_{0,mean}$  - Mean value of modulus of elasticity in the longitudinal direction  
 $E_{90,mean}$  - Mean value of modulus of elasticity in the transverse direction  
 $G_{0,mean}$  - Mean value of shear modulus  
 $G_{90,mean}$  - Mean value of rolling shear modulus  
 $I_{x,net}$  - Net moment of inertia with rotation about the  $y$ -axis  
 $I_{y,net}$  - Net moment of inertia with rotation about the  $x$ -axis  
 $J$  - Amount of force in percent distributed on a specific support  
 $K_{ser}$  - Slip modulus  
 $L$  - Diaphragm length

## Latin lower case letters

$b$  - Board width  
 $b_x$  - Board width in  $x$ -direction  
 $d$  - Screw thread diameter  
 $d_{ef}$  - Effective screw diameter  
 $d_n$  - Screw inner thread diameter  
 $f_{h,\theta}$  - Embedment strength of a screw at an angle to the grain  
 $f_{m,k}$  - Characteristic bending strength  
 $f_{t,0,k}$  - Characteristic tension strength parallel to grain  
 $f_{t,90,k}$  - Characteristic tension strength perpendicular to grain  
 $f_{c,0,k}$  - Characteristic compression strength parallel to grain  
 $f_{c,90,k}$  - Characteristic compression strength perpendicular to grain  
 $f_{v,0,k}$  - Characteristic shear strength in longitudinal direction  
 $f_{v,90,k}$  - Characteristic shear strength, rolling shear (transverse direction)  
 $f_{v,CLT}$  - Shear strength for a CLT-panel  
 $h_{CLT}$  - Height of CLT-panel  
 $h_x$  - Sum of the heights of boards oriented in  $x$ -direction  
 $h_y$  - Sum of the heights of boards oriented in  $y$ -direction  
 $k_{ax}$  - Axial slip modulus  
 $k_1$  - Relative elastic stiffness for lateral loading  
 $k_2$  - Relative elastic stiffness for lateral and axial loading  
 $k_{cr}$  - Cracking factor for shear load capacity  
 $k_x$  - Shear correction factor in  $x$ -direction  
 $k_y$  - Shear correction factor in  $y$ -direction  
 $k_s$  - Reduction factor for the in-plane shear stiffness of the panel  
 $k_{90}$  - Reduction factor for the embedment strength with angle between load and grain direction

$l_{ef}$  - Effective length  
 $l$  - Length of screw  
 $n_i$  - Number of partitions, one less than number of supports  
 $q_{p(z)}$  - Peak velocity pressure  
 $q_k$  - Characteristic wind load  
 $q_d$  - Design wind load  
 $t$  - Board thickness  
 $w_{middle}$  - Deflection at mid-span  
 $x_1$  - Reduced length of screw due to bending of screw

### **Greek letters**

$\alpha$  - Angle between screw and horizontal axis in  $xy$ -plane  
 $\beta$  - Angle between screw and horizontal axis in  $yz$ -plane  
 $\gamma$  - Shank to external grain angle  
 $\gamma_d$  - Partial safety factor for building element  
 $\gamma_M$  - Partial factor for material properties  
 $\theta$  - Angle between thread and grain  
 $\rho_k$  - Characteristic density  
 $\rho_m$  - Mean density

# Contents

<b>Abstract</b>	<b>I</b>
<b>Sammanfattning</b>	<b>III</b>
<b>Acknowledgement</b>	<b>V</b>
<b>Symbols</b>	<b>VII</b>
<b>1 Introduction</b>	<b>1</b>
1.1 Background . . . . .	1
1.2 Aims and objective . . . . .	3
1.3 Method and outline of report . . . . .	4
1.4 Limitations . . . . .	4
<b>2 Theoretical background</b>	<b>5</b>
2.1 Structure and properties of timber . . . . .	5
2.2 Cross Laminated Timber . . . . .	7
2.2.1 Composition . . . . .	7
2.2.2 Properties . . . . .	8
2.3 Diaphragm action . . . . .	11
2.4 Floor to floor connections . . . . .	12
2.4.1 Butt joints . . . . .	12
2.4.2 Lap joint connection . . . . .	13
2.4.3 Interlocking spline connection . . . . .	14
2.5 Finite element method . . . . .	15
2.5.1 Internal forces . . . . .	15
2.5.2 Shell elements . . . . .	15
2.5.3 Timoshenko beam theory . . . . .	18
<b>3 Methods and models</b>	<b>19</b>
3.1 Analytical models for shear stiffness in connections . . . . .	19
3.2 Assumptions for further modeling . . . . .	24
3.2.1 Diaphragm . . . . .	24
3.2.2 Connections . . . . .	24
3.2.3 Lateral loading . . . . .	27
3.3 Numerical modeling for CLT Diaphragms . . . . .	28
3.3.1 Creating the model . . . . .	28
3.3.2 Support, hinges and loads . . . . .	28
3.3.3 Laminate . . . . .	29
3.3.4 Extracting results . . . . .	30
<b>4 Results</b>	<b>33</b>
	<b>IX</b>

4.1	Analytical models for shear stiffness in connections . . . . .	33
4.2	Numerical modeling for CLT diaphragms . . . . .	33
4.2.1	Study of convergence . . . . .	33
4.2.2	Lateral displacements . . . . .	35
4.2.3	Lateral reaction forces . . . . .	38
<b>5</b>	<b>Discussion</b>	<b>47</b>
5.1	General discussion . . . . .	47
5.2	Analytical results . . . . .	47
5.3	FE-model . . . . .	48
5.4	Challenges in the project . . . . .	50
<b>6</b>	<b>Conclusion</b>	<b>51</b>
6.1	Project conclusions . . . . .	51
6.2	Future work . . . . .	52
	<b>References</b>	<b>53</b>
<b>A</b>	<b>Appendix</b>	<b>55</b>

# 1 Introduction

The chapter presents the general context of this project together with the historical background of timber construction. Thereafter, the aims and objectives of the work are outlined, followed by a presentation of the method and limitations of the project.

## 1.1 Background

Timber buildings have been constructed in various cultures for a long period. Each culture has had its own construction technique and types of connection. Wood in constructions was commonly used before modern material came into use. The timber constructions created a shelter for humans and the possibility to utilize the space indoors [5]. In the early 20th century, timber constructions declined in Europe. This was partly due to implementation of economically efficient mineral based solid materials, such as concrete and brick. Since then, timber has predominantly been used in lightweight constructions as well as during the erection phase of residential buildings [4]. At the turn of the 21st century, timber buildings recaptured parts of the market once more when concrete in multi-storey residential, office and school buildings was increasingly replaced with timber. This change was partly due to the introduction of cross laminated timber (CLT), illustrated in figure 1.1, which introduced a new (quasi-rigid) timber product to the market [4]. CLT was introduced in Europe in 1990 and reached the Swedish market in the late 1990s. The implementation of CLT as a building material has rapidly increased in Europe since 2005 [3]. In Sweden, there are currently four suppliers of CLT, with an annual production of around 200,000  $m^3$ . Globally, the demand for CLT is increasing each year [3].

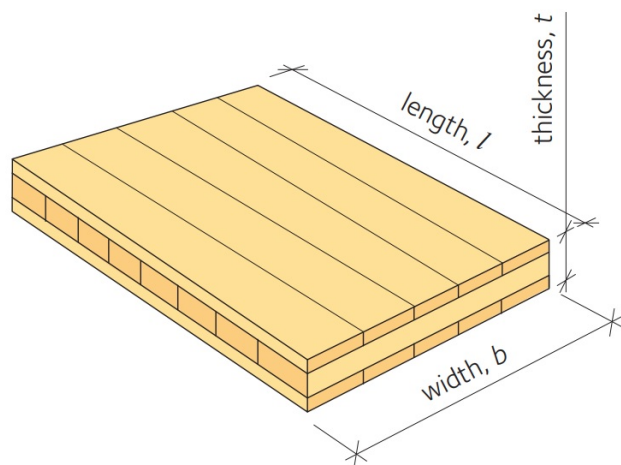


**Figure 1.1:** Cross laminated timber product (reproduced with permission from Swedish Wood from the CLT Handbook, (2019) [3])

About 1/5 of greenhouse gases released in Sweden come from the building industry. Some of the measures proposed to minimise the impact from this area are the reduction of material use, smarter production from a climate perspective and the shift to sustainable materials [18]. The use of CLT-elements in buildings can positively impact the industry and reduce the volume of emissions released since CLT consists of wood, which is a fully renewable and recyclable material. Furthermore, CLT has a long service life if the product is applied correctly in constructions [3]. This means that the material can be salvaged when such a building is demolished and used in new constructions. It can even be converted to energy through incineration [3]. Consequently, the use of CLT in construction can significantly influence the volume of greenhouse gases released by the industry and thereby minimise the impact of the sector.

Timber has complex properties due to being an orthotropic material. This implies that the properties vary depending on the orientation of the fibres. The impact of anisotropy can be reduced by implementing cross laminated timber. CLT elements are strong and stiff which can be useful in diaphragms, utilized as part of the bracing against horizontal forces in structures. Structural elements are connected to each other, which can be done in various ways. One type is presented in figure 1.2. The connections can vary from both a structural perspective by the number of fasteners, the build-up of the connection, and the material used for the connection. For CLT, the connections applied depend on the element, and the build-up governs how the element can transfer forces.

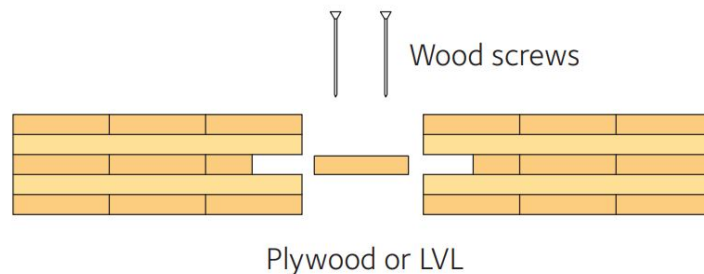


**Figure 1.2:** Example of how two CLT diaphragms are connected between on another (Reproduced with permission from Swedish Wood from the CLT Handbook, (2019) [3])

CLT elements can be created with quite sizeable cross-section giving the elements a high stiffness and a good load-bearing capacity. The production of CLT is versatile not only in cross section but also in shape since both straight and curved structural components can be produced. Wood has low self-weight and is therefore easy to transport and assemble on the building site and does not need complex foundations for timber constructions [3]. The low self-weight can thereby have a positive economic impact and increase safety through lighter elements used.

When constructing tall buildings, lateral forces from wind and earthquakes significantly affect the stability of the building. The impact on constructions from such forces can be handled by diaphragm action illustrated in figure 1.3. The term describes utilization of diaphragms of a specific material, transferring horizontal loads through itself

to the supports, which distribute the loads down to the foundation. Such action is an integral part of bracing structures. Diaphragms are elements used in floor and wall constructions and are affected by shear forces and normal forces, amongst others. Since the diaphragms transfer horizontal forces to supports, it is implied that the connections between elements and supports have an impact on the stability of the structure. For diaphragms of CLT, common connections vary from a structural perspective and performance perspective. The in-plane shear stiffness of the CLT elements and the shear stiffness of the connections between the elements govern the total stiffness of the diaphragm. The diaphragm's stiffness largely affects the ability to resist the planar shear load and distribute the load in the structures. The performance of the timber depends on the connection used between the section and consequently, it is crucial to determine the performance of CLT-diaphragms depending on the connections used.

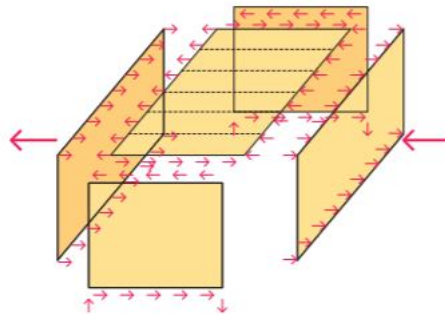


**Figure 1.3:** Illustration of how diaphragms interact in diaphragm action (Reproduced with from Swedish Wood from the CLT Handbook, (2019) [3])

## 1.2 Aims and objective

The main aim of this master's project is to determine the effect that different connections have on the in-plane shear stiffness of CLT diaphragms composed of several elements which are mechanically joined. Some sub-targets studied are stated below.

- What types of connections are presently applied for laterally loaded CLT-diaphragms?
- How does the element stiffness and connection shear stiffness affect both displacements and distribution of reaction forces in CLT-diaphragms?
- How do the different types of connection contribute to connection shear stiffness?

Since CLT is relatively new on the market, a better understanding of the mechanical characteristics could lead to a broader adaptation of the material usage in multi-storey buildings. As a result, a completely renewable material such as wood can hopefully replace the use of other materials and consequently minimise the impact on our climate that is caused by the building industry.

## 1.3 Method and outline of report

A literature review is conducted, which considers the material properties of wood, the composition of CLT and their structural benefits. Additionally, the effects and demands regarding diaphragm action are studied, as partially presented above. The main focus of the literature review is the types of connections commonly used for CLT elements and models for connection stiffness and load-bearing capacity, which are presented in chapter 2. To give an understanding of the numerical method later on, a literature review is also done in chapter 2, for the finite element method applicable to diaphragms.

Both numerical- and analytical models are defined in chapter 3. The models are based on the literature review, for the different connections and their respective parameters. Calculations for the numerical models are undertaken in a 3D finite element analysis software for structural analysis called RFEM. The software is used to create a model representing part of a floor in a residential building. The numerical model is partly based on input from the analytical models, dimensions defined in the project and partly based on the authors assumptions of a real construction. The software is used to analyze the displacements in the floor depending on lateral loads, connection stiffness and diaphragm stiffness, as well as to study the force distribution on the supports.

Lastly, results from both the analytical and numerical calculations are analysed and illustrated in chapter 4, mainly through figures and tables. These are compared and discussed in chapter 4 and 5. Finally, the conclusion is presented in chapter 6, together with a discussion on the potential future applications of the research.

## 1.4 Limitations

The project focuses on the effect that shear stiffness in the connections and element stiffness have on deflections and force distribution in a floor structure consisting of CLT-panels. Therefore, no contribution from either moisture or temperature variation will be considered in the results. The moisture and temperature are assumed as constant. A further limitation is imposed by considering any potential cracks in boards as non-existing and therefore not subject to moisture intrusion. In addition, the diaphragms studied in this project are not designed with cuts for stairs, elevators or any other technical or aesthetic aspect.

Another explicit limitation is the connections. There exist many commonly used types of connections applied for CLT today. To avoid any confusion, the project focuses on a specific number of commonly used connections for the case of lateral loading. Vertical loading and the effects from such forces are neglected in the study. Buckling or any initial deformation of the floor diaphragm is not considered during any part of this project.

## 2 Theoretical background

This chapter outlines the theoretical background of the project, including the structure of timber and CLT and the material properties of CLT. Subsequently, this section is followed by a theoretical study on floor-to-floor connections, diaphragm action and the theory behind the chosen calculations and modeling.

### 2.1 Structure and properties of timber

In Sweden, the most common species of trees used for construction are spruce and pine. Birch and other deciduous species are also found in the forest but not used as construction material to any significant extent [2].

The internal structure is similar between spruce and pine and centres around a pith in the middle of the stem, running along the whole tree. The wood enclosing the pith is characterized by two different types, heartwood and sapwood. As can be seen in figure 2.1 heartwood has a darker colour whereas sapwood is of lighter colour. The difference in colour is valid for pine. In the case of spruce, the difference is not visible [22]. The cambium and bark surround the inner wood. Each year the tree enlarges during the growth season. In the transverse direction, the growth takes place in the cambium where new cells are formed. During the spring and early summer, short and wide cells are formed, which have a low density and result in a wood called earlywood, the "springwood". However, in the months of summer, the cells formed are longer with thicker cell walls resulting in higher density, known as latewood. The proportion of latewood affects the density of the wood [22]. The fibres in wood are long, hollow cells oriented in the longitudinal direction. In timber, the directions are divided into a longitudinal, tangential and radial direction depending on the cross-section [2]. As can be seen in figure 2.2, the longitudinal direction follows the fibres. In contrast, the tangential direction follows the curvature of the annual ring, whereas the radial direction crosses the annual rings orthogonally from pith to bark. The orientation of the fibres correlates to the properties of wood [22].

Stiffness is a characteristic of timber that indicates the elasticity of the material [16]. The stiffness of a material is coherent with the modulus of elasticity (MOE), with a high MOE meaning high stiffness [22]. One of the main focuses of the project is the shear stiffness, which according to [16] instead is coherent with the shear modulus. A stiff diaphragm minimises the effects of creep and the initial deformation from a constant vertical load [22]. If wood is exposed to temperatures above 95°C for a short time or temperatures above 65°C during a long period, the consequence is loss of both stiffness and strength due to thermal degradation [2].

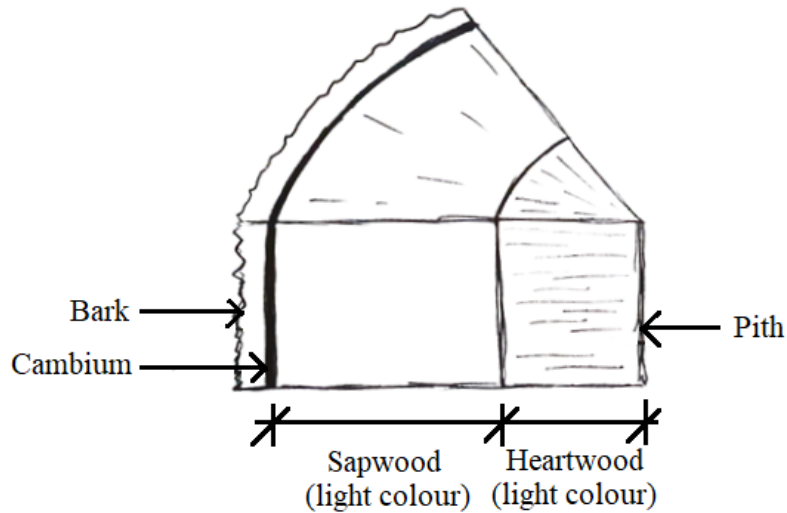


**Figure 2.1:** Internal structure of a tree

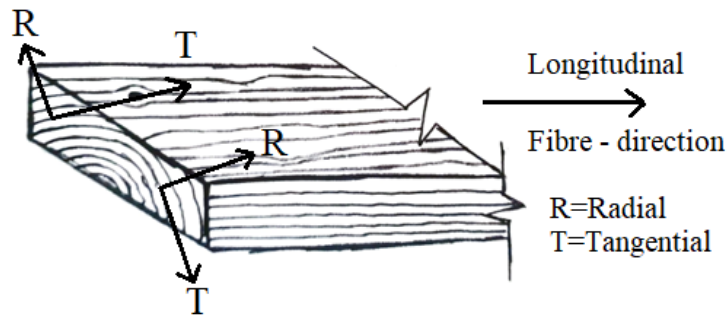


**Figure 2.2:** Material principal directions of a sawn timber board

The strength- and stiffness values are higher for small clear specimens. Due to imperfections such as knots or other defects, sawn timber have less capacity. Structural timber exhibits the highest characteristic strength when loaded in bending parallel to the fibre direction. C24 timber loaded in tension parallel to the grain has a characteristic strength of 14.5 MPa and merely a value of 0.5 MPa when loaded in tension perpendicular to the grain. In the case of compression, the characteristic strength when loaded parallel to the grain is determined as 21 MPa. When compressed perpendicular to the grain, the characteristic strength is 2.5 MPa. The mean stiffness for strength class C24 timber when loaded parallel to the grain is 11000 MPa, 370 MPa when loaded perpendicular to the grain and C24 has a mean shear modulus of 690 MPa [12]. Timber has different shear capacity depending on the direction of the shear loading, which is illustrated in figure 2.3. The most common cases of shear loading in timber structures are the longitudinal-radial and longitudinal-tangential direction [2].

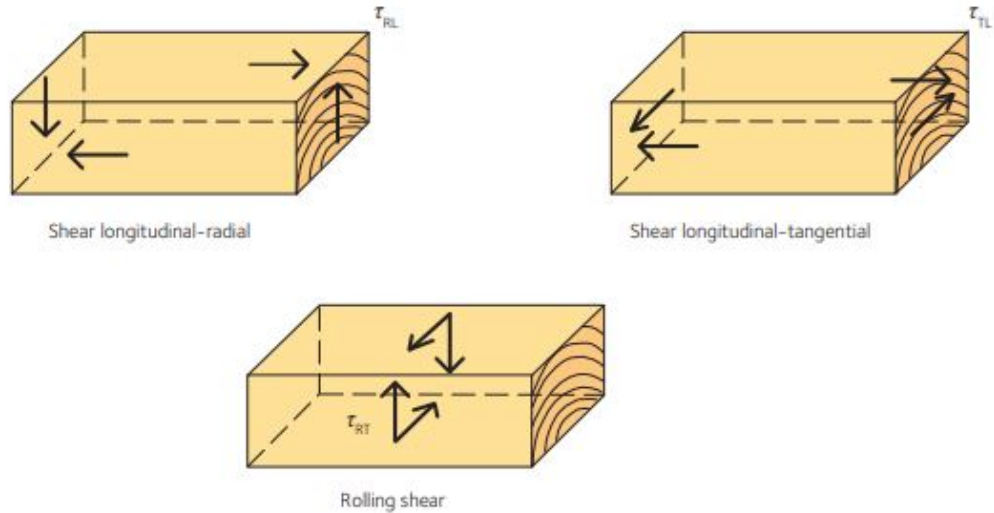


**Figure 2.3:** Shear forces in timber depending on direction (Reproduced with permission from Swedish Wood from Design of timber structures Volume 1, (2016) [2])

## 2.2 Cross Laminated Timber

This section explains the structure of CLT, the structural benefits of CLT for construction and a selection of changes in material properties due to composition.

### 2.2.1 Composition

Cross laminated timber (CLT) is a timber product and has a specific composition, unlike other timber products. As seen in figure 2.4, CLT is comprised of an odd number of layers such as three, five and seven layers, but should be at least three layers. Each layer consists of laminations glued together crosswise at a  $90^\circ$  to adjacent layers. The laminations are made up of boards that are joined with glue [23]. According to the supervisor, the face sides are joined through glue, whereas the edge sides are not glued. The result is a homogeneous laminar composite element with the layers having a orthogonal orientation [23].

If used as panels, most of the stress caused by internal and external loading occurs in main direction, which commonly corresponds to the longitudinal direction of the top layer. This is mainly due to the longitudinal direction exhibiting a higher stiffness compared to the transverse direction [23]. In some cases, the quality of timber boards used for layers varies in the panels. To utilize the strength of the composition and timber, the odd numbered layers corresponding to the main direction often have the same and slightly higher strength compared to the even layers. Stresses are usually more significant in the main direction, and thus, slightly higher quality timber could be placed in these areas to manage the stress [2].

For connecting the boards and layers, two different adhesives are applied in current use. These are polyurethane (PUR) and melamineurethane-formaldehyde (MUF) [23]. The moisture content in CLT-elements is governed by the type of glue used. During the process of joining boards, the moisture content should not be less than 8% and

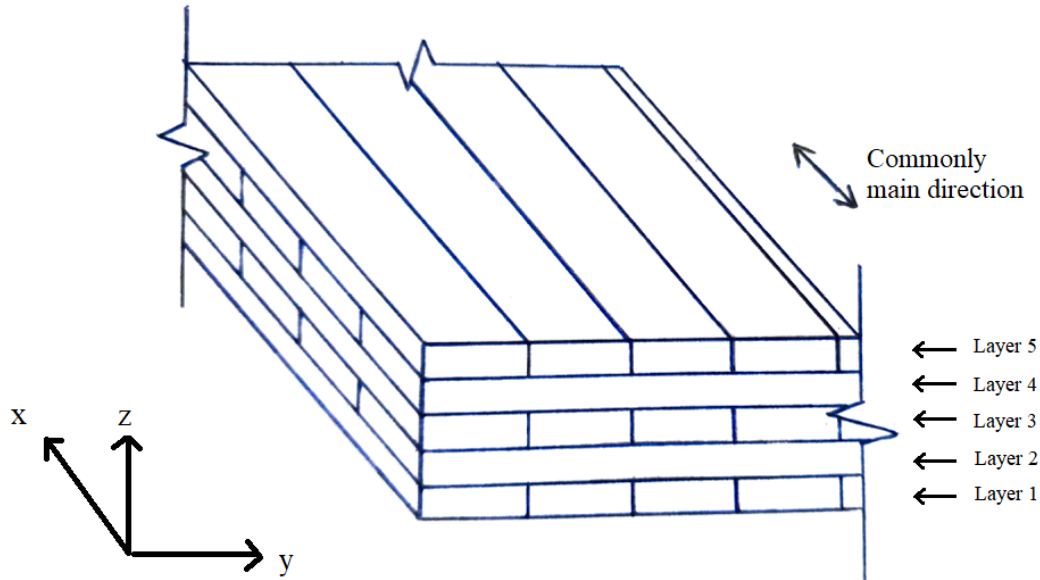


**Figure 2.4:** Composition of a CLT element

not exceed 15%. In the final product, the variation of moisture content in between boards should not be more than five percentage points [3].

CLT is manufactured in various dimensions, with a board width spanning from 40 to 300 mm and board thickness measuring between 6 and 45 mm. The total length when manufacturing one element can reach 16 m [23]. However, the maximum length can be extended to 30 m [2]. The standard thickness of timber boards is between 20 to 45 mm with a width between 80 to 200 mm and a classified strength between C14 and C30 [2]. The standard thickness of a CLT panel spans up to 300 mm but can be made up to 500 mm if requested [23].

## 2.2.2 Properties

The properties of timber vary depending on the orientation of fibres. Such material is known as an anisotropic material. In this section, both physical and mechanical properties of CLT are introduced.

The density is relatively low compared to other construction materials. Though having a lower density, the strength in relation to the weight is high, giving CLT a high load bearing capacity [3]. The characteristic density used for CLT panels of C24 timber boards and the mean density are presented in table 2.1.

The stiffness and strength of CLT are greatly dependent on the direction of loading relative to the fibre orientation. It affects both the mechanical behaviour from compression, tension or a combination of the two within the boards [22]. Values for the stiffness and strength parameters are presented in table 2.1. CLT exhibits highest stiffness in the longitudinal direction and lowest in the transverse direction. In the

transverse direction, the mean value varies. CLT has a lower stiffness for panels made without edge-glued boards and higher stiffness for those with edge-glued boards [3]. Regarding the two different shear moduli, CLT has a lower value for the rolling shear modulus compared to the longitudinal shear modulus. Regarding the shear capacity, values does not vary for shear in the longitudinal-radial and shear in the longitudinal-tangential direction, but varies if the CLT-element is subjected to rolling shear. Values for shear capacity are shown in table 2.1.

Since the layers are rotated 90 degrees, the longitudinal direction of the top layer corresponds to the transverse direction of the layer beneath. The longitudinal direction of the layer beneath corresponds to the top layers transverse direction [3]. This means that the mean shear modulus in the global x-direction of the top layer corresponds to the mean shear modulus in the global y-direction of the layer beneath, as illustrated in figure 2.5. The top layer has a mean modulus of rolling shear in the global y-direction which corresponds the the mean modulus of rolling shear of the layer beneath in the global x-direction.

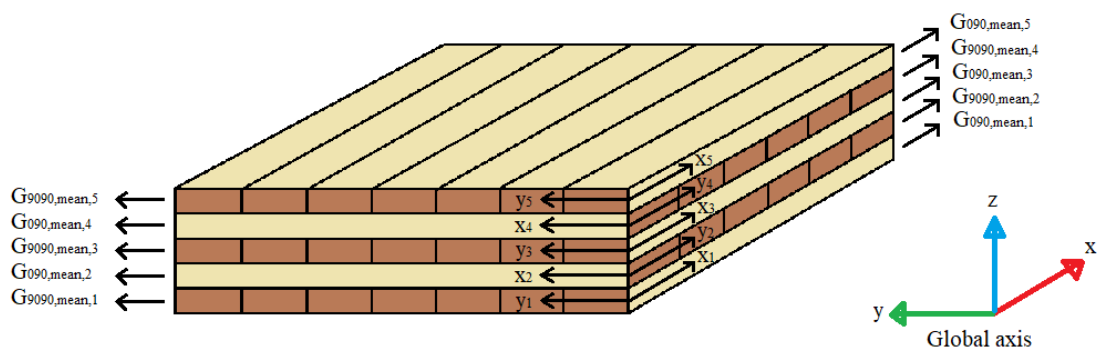


**Figure 2.5:** Illustration of the shear modulus, rolling shear for the different layers in a 5-layered CLT panel with the local axes in the panel and global axes outside

CLT-panels loaded in compression and tension display values presented in table 2.1. In the case of both compression and tension when loaded parallel to the fibre direction, the wood within CLT elements displays a relatively good characteristic strength for CLT panels with C24 classified timber boards [3] with higher strength in compression compared to tension. When loaded in tension, the failure is brittle when the capacity is reached [2]. CLT-panels loaded in compression parallel to the plane has buckling of fibre as the usual cause of failure [2]. The characteristic strength when loaded perpendicular to the fibre direction, both in compression and in tension, is considerably lower for panels of strength class C24 timber compared to when loaded parallel to the fibre direction. When loaded in compression perpendicular to the grain, the cells in the wood are crushed. The material can still carry forces, but the stiffness and strength for this case is low [2]. The cause of failure when fibres are being pulled apart, as tension perpendicular to the plane, requires a lower force than when pulled parallel [2].

Several factors affect the strength of CLT. According to [2], the strength of the timber in CLT seems to decline when loaded with a force during an increased time. The

strength is also partly dependent on the density of wood [22]. Another parameter affecting the magnitude of strength is the content of moisture. As a consequence, strength of CLT declines with both increased load duration and increased moisture content [2].

Differences in the build-up and material strength results in varying resistance of CLT. Therefore, the resistance is dependent on the exact composition of the elements. The effects from load duration and moisture are for structural design reasons considered by the use of modification factors that analyse any effects these parameters may have on CLT [23]. It is important to know that CLT properties can vary within one component and between different elements [3].

**Table 2.1:** Material properties of CLT panels with C24 boards given in [3]

	Value	Unit
Characteristic density, $\rho_k$	350	kg/m <sup>3</sup>
Mean density, $\rho_m$	420	kg/m <sup>3</sup>
Mean modulus of elasticity longitudinal direction, $E_{0,mean}$	11000	MPa
Mean modulus of elasticity transverse direction, $E_{90,mean}$	0 <sup>1</sup> or 400 <sup>2</sup>	MPa
Mean shear modulus, $G_{090,mean}$	690	MPa
Mean modulus of rolling shear, $G_{9090,mean}$	50	MPa
Tension strength in plane, $f_{t,0,k}$	14.5	MPa
Tension strength perpendicular to the plane, $f_{t,90,k}$	0.4	MPa
Compression strength in plane, $f_{c,0,k}$	21	MPa
Compression strength perpendicular to the plane, $f_{c,90,k}$	2.5	MPa
Shear strength, $f_{v,CLT}$	4.0	MPa
Rolling shear strength, $f_{v,9090}$	1.1 <sup>3</sup> or 0.7 <sup>4</sup>	MPa

1 - Used for CLT panels without edge-glued boards

2 - May be used for CLT panels with edge-glued boards

3 - Used for CLT panels with edge-glued boards or where the board thickness is less than 45 mm and the width to thickness ratio for the boards is equal to or greater than 4

4 - Used for CLT panels where the boards are not edge-glued and where the width to thickness ratio for the boards is less than 4, or where grooves have been cut into the boards.

## 2.3 Diaphragm action

Stabilizing structures against horizontal forces is important. When constructing buildings with few storeys, the horizontal forces caused by wind can be assumed to be constant across the height but not for multi-storey buildings. Bracing systems are applied to handle these forces. There are mainly three different types of systems applicable. The first is lacing, which can be applied as crosses from one floor to the one below or as a single system. Both cases are illustrated in figure 2.6. The second is moment stiff connections made between beam and column or between column and foundation. The last one is diaphragm action. Since this project is focused on diaphragm action, this will be evaluated in further detail.

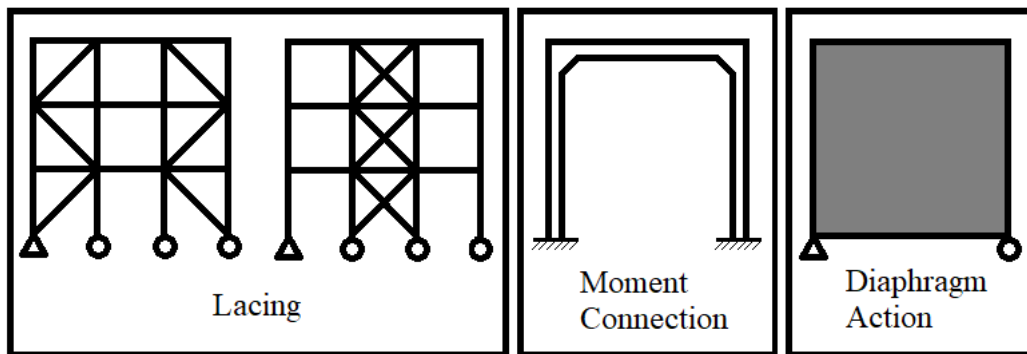


**Figure 2.6:** Illustration of lacing, diaphragm action and moment connection

Diaphragm action stabilises the system against horizontal forces and distributes them in the plane [20]. The sum of the forces acting on each storey above the section and half of the storey below can be used to determine the impact on the section [23]. With increasing height of buildings, the importance of stabilizing a structure against lateral forces is crucial. When constructing timber multi-storey buildings made entirely of wood, CLT is the most common product used as a diaphragm [21]. In buildings of a larger size, the system must be complemented with additional bracing. This can be made with lacing made from steel braces. One prerequisite to ensure diaphragm action is that the diaphragms are thick enough to avoid buckling of the element [20]. The bracing elements should be placed equally on each floor and at every storey along the height of the building to avoid a different centre of gravity and thereby also avoid torsion. Diaphragms on every floor creates a continuous diaphragm action, which is essential to make sure that the impact from loads is transferred to the foundation. The regular arrangement of the diaphragms in the floor can improve the stabilisation against effects from earthquakes [23].

Loading in the longitudinal direction of the diaphragm results in shear forces ( $T_d$ ) and flange forces ( $D_d$  and  $Z_d$ ) in the diaphragm, which can be viewed in figure 2.7. Shear forces must be taken into account in the initial design and must be handled by fasteners in-between the diaphragms. Often the lateral forces can vary, and therefore the sign and alternate direction of horizontal forces should be take into account [23]. Since the shear forces in the diaphragms must be handled by the connections in between panels, it is important to ensure enough stiffness in the connections between diaphragms.

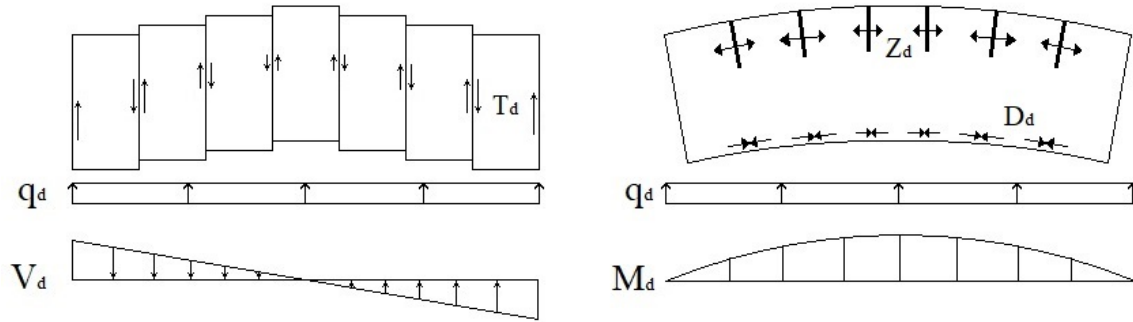


**Figure 2.7:** Illustration of shear forces between elements (left) and flange forces along the edges (right) (inspired by illustration from ProHolz from Koppelhuber, Pock and Wallner-Novak, (2014) [23])

## 2.4 Floor to floor connections

The build-up of cross laminated timber presents a practical option of joining together panels. CLT elements can be connected to the surface of the narrow sides [23]. Self-tapping wood screws can then be used to fasten the elements with versatility and a high speed during installation [17]. The screws connect the panels to handle forces acting in the connection as illustrated in figure 2.8.

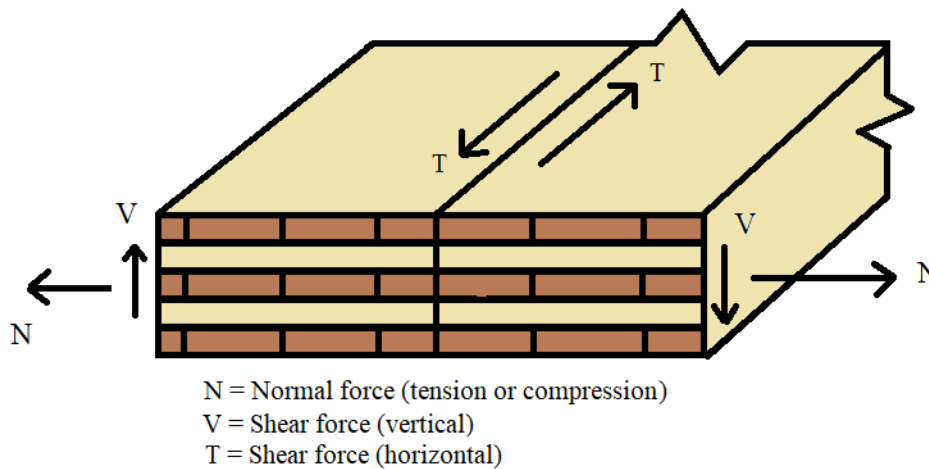


**Figure 2.8:** Flow of forces in a connection

### 2.4.1 Butt joints

From a production perspective, the simplest connection to manufacture is the butt joint connection [24]. As shown in figure 2.9, this type of connection consists of two edges which are cut straight and connected with self-tapping screws at an angle to the grain. The result of matching cut elements when using butt joints, is that the connection requires less material and the panels can be assembled faster in fabrication. Screws are installed from both sides with the penetration of the shear plane usually done at the middle board. The inclination of the screws results in stiffer connections

and can also handle greater loads compared to orthogonally installed screws. Butt joints can be applied for panels with a thickness of around or more than 100 mm thickness due to penetration requirements [17]. Normal and shear forces are transferred between diaphragms by the screws.

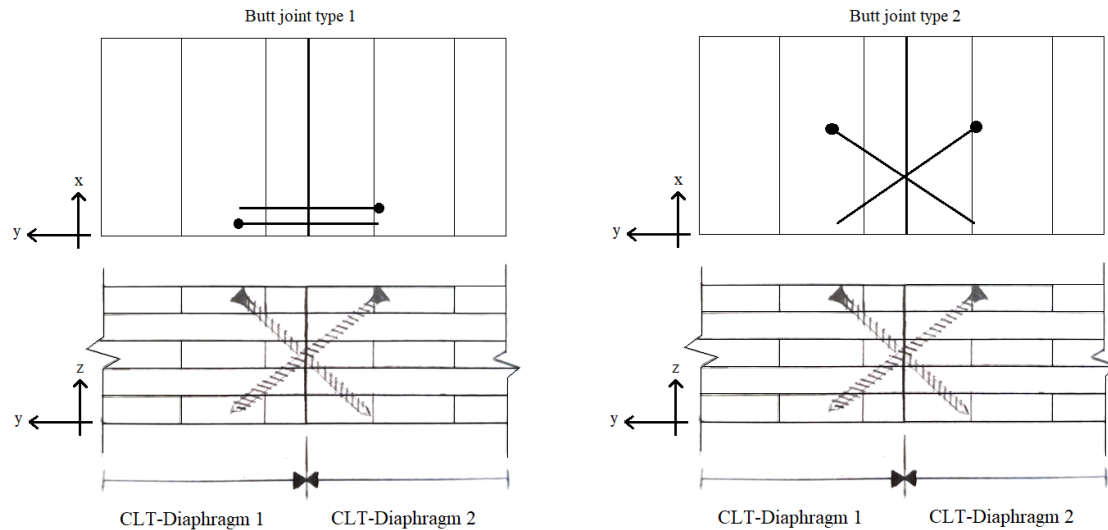


**Figure 2.9:** Illustration of a two different types of butt joint connections

### 2.4.2 Lap joint connection

Compared to the butt joints, lap joints are not as simple to produce. A lap joint, shown in figure 2.10, consists of two diaphragms connected by self-tapping screws. One of the diaphragms has part of the thickness removed from the top, and the other has part of the thickness removed from the bottom. The panels are then connected with screws intersecting the shear plane in the centre of the panel thickness. For the type of connection illustrated in figure 2.10, the screws are installed orthogonally to the plane [17]. The screw in a lap joint can transfer both normal forces and shear forces between diaphragms. Due to no inclination of the screw in the model in figure 2.10, the capacity of the joint is limited by the shear strength of the screw to handle normal and horizontal shear forces.

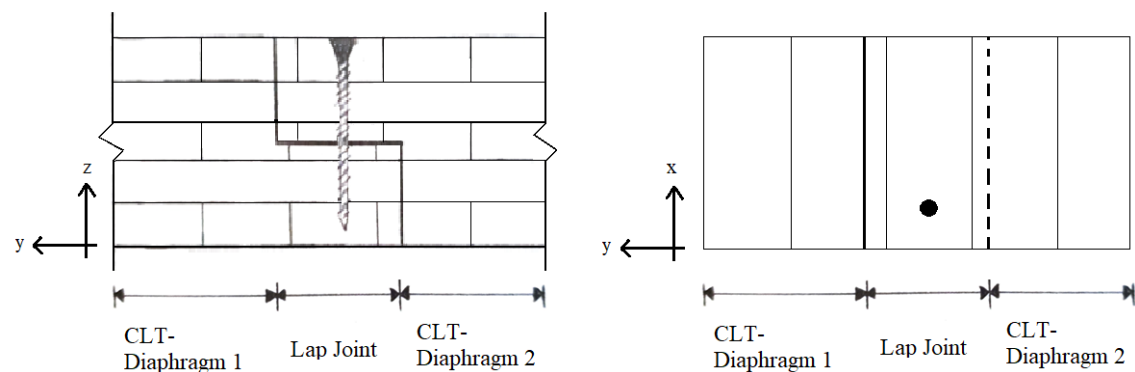


**Figure 2.10:** Illustration of a Lap joint connection

### 2.4.3 Interlocking spline connection

Interlocking spline connections are alike butt joints, but as seen in figure 2.11, instead of straight edges, part of a single or double layer on both panels can be exchanged for a spline placed instead of the removed part. The spline can be made from plywood, steel or planed timber [3]. When designing spline connections, the screw bearing strength of plywood is important to take into account to ensure sufficient connection since it usually has a low bearing strength [17]. The screws mostly handles the normal- and horizontal shear forces whilst the spline are subjected to all forces. This composition has different names depending on the number and placement of plywood splines.

If part of the middle layer of the CLT-panels are exchanged, the joint is called a "joint with a loose tongue", as shown to the left in figure 2.11. The panels can then be connected either with screws or nails. This connection transfers forces both across and along the plane of a CLT-panel.

If part of the top and/or bottom layer board is exchanged, the joint is called a "joint with a single or double cover plate". Like the connection with a loose tongue, the connection can utilise screws or nails to connect the panels. The connection has orthogonal screws through the spline, illustrated in figure 2.11. Joints with cover plates can transfer shear forces, tensile and compressive forces in the plane [3], as seen in figure 2.8 in section 2.4.

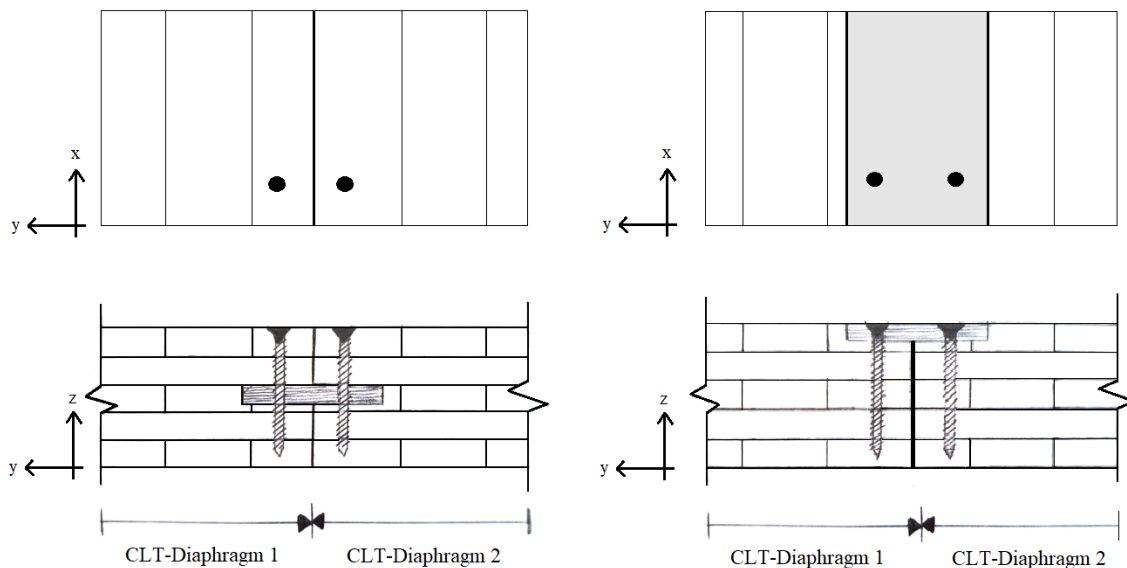


**Figure 2.11:** Illustration of spline connection with a loose tongue to the left and with a single cover plate to the right

## 2.5 Finite element method

This chapter explains the relevant theory of the finite element method behind the modeling in the case study. Within this project floor diaphragms are considered, and therefore this chapter focuses on the finite element method applied to diaphragms and the connections between such elements.

### 2.5.1 Internal forces

CLT has a low torsional stiffness which results in internal forces. Due to complexity of the effect from torsional stresses, CLT-panels can be assumed as fully flexible regarding torsional flexibility. The result of such assumptions is conservative as it gives slightly higher deflections and bending moments to account for when designing the panels [1]. Bending moments, shear forces and normal forces in the diaphragm and the direction of the forces can be studied for an arbitrary section of a CLT-diaphragm in figure 2.12. The direction of  $x$  is the same as the longitudinal direction of the top layer,  $y$  is transverse to this direction and  $z$  is directed along with the thickness of the element.

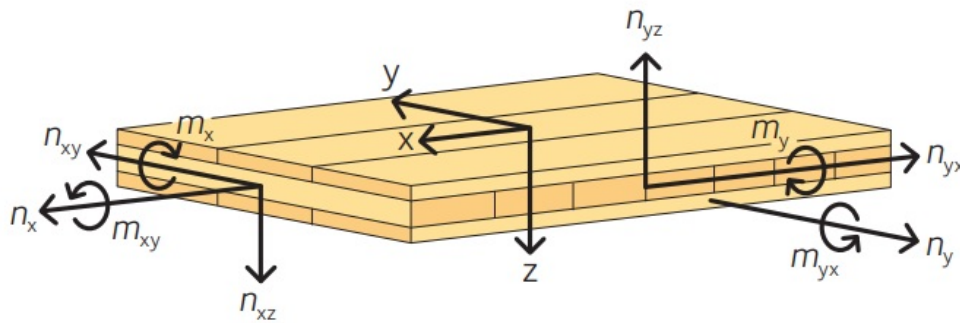


**Figure 2.12:** Internal forces in a two-dimensional structural element (reproduced with permission from Swedish Wood from the CLT Handbook, (2019) [3])

### 2.5.2 Shell elements

As explained in earlier chapters, CLT is an orthotropic product even if the layout minimises the effect. The material's behaviour depends on the direction of the layer where forces are applied, and so does the deformation. In the case of CLT panels, shear deformations in-plane must be considered. However, there is no need to study the effects of longitudinal stressing at the same time as transverse stressing [1]. Shell elements are a combination of plate and plane stress elements [19].

From [1], it is stated that CLT is best modelled according to the Mindlin-Reissner elements since they can be modelled as two-dimensional equivalent elements of the Timoshenko beam theory and consider the shear deformations in the material [1]. The Kirchhoff plate theory is not applicable to thicker plates with shear strains. Instead, the Mindlin-Reissner plate theory is used [19]. In order to determine the correlation between strains and internal forces in the material, the stresses of shell elements need to

be determined. With these known, a matrix for Mindlin-Reissner elements illustrating the strains and internal forces can be set forth as seen in equation 2.12, which is illustrated in [3]. All the equations in the matrix below are presented by Borgström, E. and Fröbel, J. in [3].

$$D_{11} = \frac{E_{0,mean} \cdot I_{x,net}}{1 - \nu_{xy} \cdot \nu_{yx}} = E_{0,mean} \cdot I_{x,net} \quad (2.1)$$

$$D_{22} = \frac{E_{0,mean} \cdot I_{y,net}}{1 - \nu_{xy} \cdot \nu_{yx}} = E_{0,mean} \cdot I_{y,net} \quad (2.2)$$

$$D_{12} = D_{21} = \sqrt{\nu_{xy} \cdot \nu_{yx} \cdot D_{11} \cdot D_{22}} = 0 \quad (2.3)$$

$$D_{33} = k_{cr} \cdot G_{0,mean} \cdot \frac{h_{CLT}^3}{12} \quad (2.4)$$

$$k_{cr} = \begin{cases} 0.65 & \text{for CLT with splits or slits} \\ 0.8 & \text{for CLT without splits or slits} \end{cases} \quad (2.5)$$

$$D_{44} = k_x \cdot G_{0,mean} \cdot h_x \quad (2.6)$$

$$D_{55} = k_y \cdot G_{0,mean} \cdot h_y \quad (2.7)$$

The heights used in equation 2.6 and 2.7 represent the sum of thickness for all the boards oriented in the same direction. The shear correction factors  $k_x$  and  $k_y$  are chosen for a 200 mm thick CLT-slab with C24 boards, and values can be seen in table 2.2 with values according to SS-EN 338.

**Table 2.2:** Shear correction factors for a 200 mm thick five-layered CLT-panel with each layer having a thickness of 40 mm and strength class C24 timber [3]

	Value [-]
$k_x$	0.194
$k_y$	0.152

$$D_{66} = E_{0,mean} \cdot h_x \quad (2.8)$$

$$D_{67} = D_{76} = 0 \quad (2.9)$$

$$D_{77} = E_{0,mean} \cdot h_y \quad (2.10)$$

$$D_{88} = k_s \cdot G_{0,mean} \cdot h_{CLT} \quad (2.11)$$

In equation 2.12, equations 2.1 - 2.4 describe the properties for bending in the panel, which correlate to the first three rows and columns. Equations 2.6 -2.7 represent the out-of plane shear stiffness for a CLT slab correlating to the fourth and fifth row and column. Lastly, equations 2.8 - 2.11 are used for the in-plane stiffness in a CLT panel, which are presented in the last three rows and columns in equation 2.12 [3]. The factor  $k_s$  is a reduction factor governing the in-plane shear stiffness of a CLT-diaphragm and can be used to both reduce and increase the stiffness during modeling of a CLT-diaphragm. Since the project considers the element stiffness, the factor  $k_s$  is a central parameter of this study and used later on.

$$C_{CLT} = \begin{bmatrix} D_{11} & D_{12} & 0 & 0 & 0 & 0 & 0 & 0 \\ D_{21} & D_{22} & 0 & 0 & 0 & 0 & 0 & 0 \\ 0 & 0 & D_{33} & 0 & 0 & 0 & 0 & 0 \\ 0 & 0 & 0 & D_{44} & 0 & 0 & 0 & 0 \\ 0 & 0 & 0 & 0 & D_{55} & 0 & 0 & 0 \\ 0 & 0 & 0 & 0 & 0 & D_{66} & D_{67} & 0 \\ 0 & 0 & 0 & 0 & 0 & D_{76} & D_{77} & 0 \\ 0 & 0 & 0 & 0 & 0 & 0 & 0 & D_{88} \end{bmatrix} \quad (2.12)$$

In equation 2.12, the normal stresses expressed for one direction in the matrix have no relation with the regular expansions in another direction. This is, for example, expressed through the calculations for the  $x$ -direction only being dependent on the moment of inertia in the  $x$ -direction. In the matrix, values in all rows and columns except for the diagonal have a value of zero [3]. Among other reasons, this can be explained by Poisson's ratio in the  $xy$ -plane and  $yx$ -plane having a value of zero [3]. According to [1], the layup for CLT formation of butt joints transverse to the main direction also impacts the neglecting of transverse expansion. According to [1], for the section shear stiffness of a slab in the matrix, the shear stiffness for a CLT-diaphragm can be determined with the mean shear modulus, the net to height and correction factors for shear, taking into account the orthotropic composition. The composition is considered in equations 2.6 and 2.7, with the net height, depending on the orientation of each layer [1]. All the equations creating the matrix are illustrated in figure 2.13 with their respective direction presented.

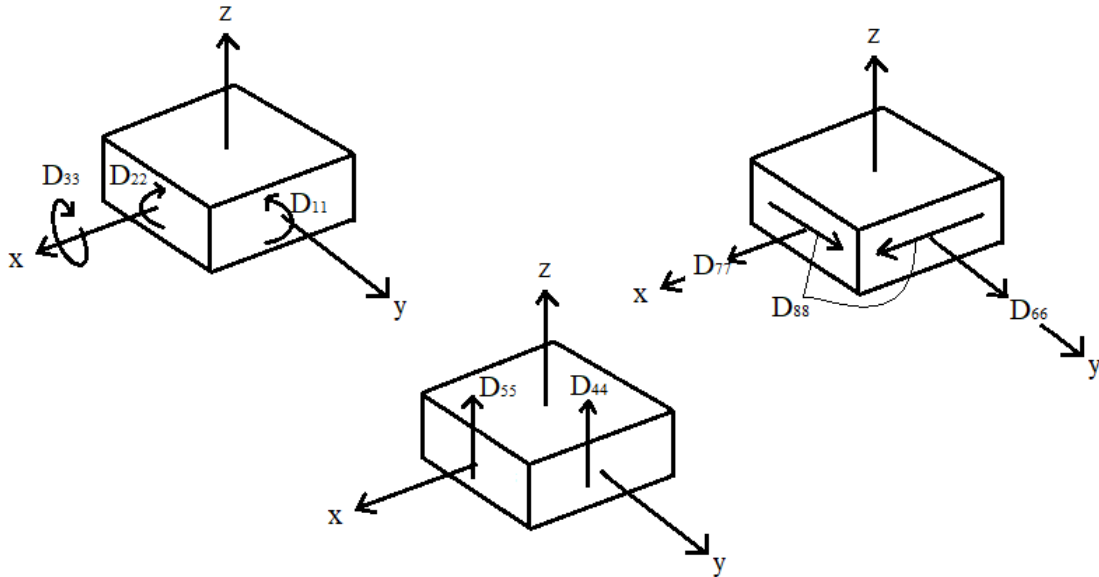


**Figure 2.13:** Bending, shear and plate forces from equation 2.12 illustrated for part of a CLT slab

### 2.5.3 Timoshenko beam theory

The Mindlin-Reissner theory mentioned in previous chapter is based on the Timoshenko beam theory. Contrary to the classical Euler-Bernoulli beam theory, Timoshenko beam theory accounts for the shear deformations of beams [1]. Further, the Timoshenko beam theory considers the rotary inertia [9]. In theory, Euler-Bernoulli theory considers the cross section to be constant when the beam deforms whereas Timoshenko beam theory accounts for the shear deformations. The result is that the deformed shape of the beam is not perpendicular to the neutral axis. According to [1], the deformations from Euler-Bernoulli beam theory is 20 to 30 percent larger than those calculated with Timoshenko beam theory. As mentioned earlier, Timoshenko beam theory is applied for thicker plates and Euler-Bernoulli is used when analyzing thinner plates [1]. The amplitude of deformation seems to follow the thickness of the panel with an increase in deformation as a result of decreasing the thickness of the plate [9].

## 3 Methods and models

The chapter presents the different methods and models. First the analytical models are introduced for three commonly used connections between CLT-diaphragms in floor constructions. Then, the assumptions for further modeling is presented followed by the method of numerical modeling.

### 3.1 Analytical models for shear stiffness in connections

For self-tapping screws where the outer thread diameter is larger than the shank diameter the effective diameter is determined according to EC5 [11]. In equation 3.1 the effective diameter is determined with regard to the inner thread diameter.

$$d_{ef} = 1.1 \cdot d_n \quad (3.1)$$

For crossed screws and inclined screws according to figure 3.1, two insertion angles are defined. These angles are used in equation 3.2 to calculate a shank to external grain angle ( $\gamma$ ) presented in [15]. The values for the insertion angles in the case of axial loading is taken from the results in [15] where the angle configuration gave good stiffness values for a butt joint connection.

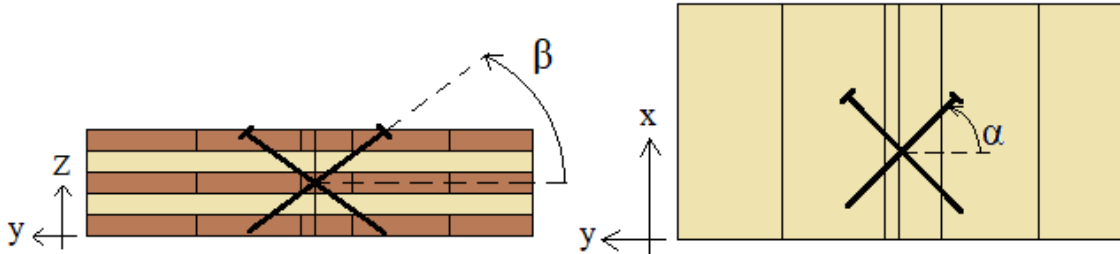


**Figure 3.1:** Illustration of the angles  $\beta$  and  $\alpha$  in a CLT-diaphragm

$$\gamma = \arccos(\cos \beta \cdot \sin \alpha) \quad (3.2)$$

For axially loaded screws the embedment strength at an angle to the grain ( $\theta$ ) needs to be determined. Since the angle  $\theta$  varies in CLT elements, a simplification is made that the angle corresponds to the difference between the thread and the grain direction in the top layer as seen in figure 3.2. The embedment strength is determined according to Loss et al [15] with the correction factor determined with equation 3.3 and then implementing equation 3.4.

$$k_{90} = 1.35 + 0.015 \cdot d_{ef} \quad (3.3)$$

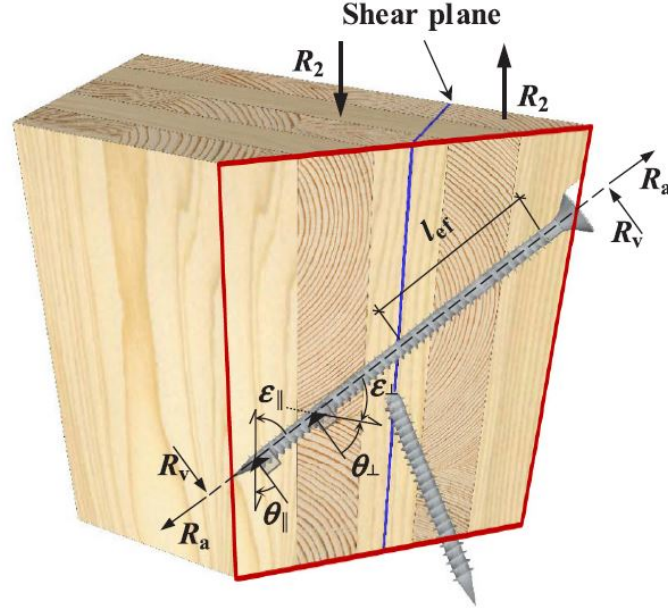


**Figure 3.2:** Illustration of the angle  $\theta$  in a butt joint connection (reproduced with permission from Elsevier Ltd from Loss, Hossain and Tannert, 2018 [15])

$$f_{h,\theta} = \frac{0.082 \cdot (1 - 0.01 \cdot d_{ef}) \cdot \rho_k}{k_{90} \cdot \sin^2 \theta + \cos^2 \theta} \quad (3.4)$$

The axial loading results in an edge effect where the screw tends to bend [15]. This effect is considered by subtracting the length with the value determined by equation 3.5 presented in [14]. The longitudinal shear strength of CLT is assumed as 4.0 MPa, taken as the shear strength of a CLT panel consisting of only strength class C24 timber according to table 3.6 in [3].

$$x_1 = \frac{f_{h,\theta} \cdot d_{ef}}{2 \cdot \tan \gamma \cdot f_{v,CLT}} \quad (3.5)$$

The effective length of axially loaded screws is thereby determined with the following equation.

$$l_{ef} = l - x_1 \quad (3.6)$$

To calculate the shear stiffness in the connection some moduli need to be determined. Today these are calculated according to a simplification in Eurocode 5 and technical approvals for screws. For lateral loading a slip modulus per shear plane is presented by Eurocode 5 in [11] with the diameter exchanged for the effective diameter in the case of self-tapping screws according to Loss et al [15] resulting in the expression given in equation 3.7.

$$\begin{aligned} K_{ser} &= \rho_m^{1.5} \cdot \frac{d_{ef}}{23} \\ \rho_m &= [\text{kg}/\text{m}^3] \\ d_{ef} &= [\text{mm}] \\ K_{ser} &= [\text{N}/\text{mm}] \end{aligned} \quad (3.7)$$

The shear stiffness in a connection with screws loaded both laterally and axially considers the axial slip modulus as well as the slip modulus. The axial slip modulus is an estimation and calculated according to technical approvals in [7] presented in equation 3.8. The equation is applied when the diameter is thicker than 6 mm and the maximal width of the gaps in the layers of the CLT panels is less than the screw's inner thread diameter [15].

$$\begin{aligned}
 k_{ax} &= 780 \cdot d^{0.2} \cdot l_{ef}^{0.4} \\
 d &= [\text{mm}] \\
 l_{ef} &= [\text{mm}] \\
 k_{ax} &= [\text{N/mm}]
 \end{aligned} \tag{3.8}$$

With the slip modulus and the relative axial slip modulus known, a relative elastic stiffness can be determined for laterally loaded connections. Depending on the insertion angles of the screws, two different calculations are applied. If the connection consists of pairs of screws connected according to the theory of parallel-connected springs and loaded only in shear, equation 3.9 is used according to [15], with a connection presented in figure 3.3. However, for a single screw, the relative elastic stiffness in shear is half the value of equation 3.9 and such connection is illustrated in figure 3.4. In the case of two screws connected in a series-connection, loaded only in shear, equation 3.10 is applied according to [6] with connection illustrated in figure 3.5. For connections with screws inclined and therefore also subjected to tension-shear and compression-shear, equation 3.11 presented in [15], is applied to determine the shear stiffness of the connection which is illustrated by the connection in figure 3.6.

$$k_1 = 2 \cdot K_{ser} \tag{3.9}$$

$$k_1 = \frac{1}{\frac{1}{K_{ser}} + \frac{1}{K_{ser}}} \tag{3.10}$$

$$k_2 = 2 \cdot (K_{ser} \cdot \sin^2 \gamma + k_{ax} \cdot \cos^2 \gamma) \tag{3.11}$$

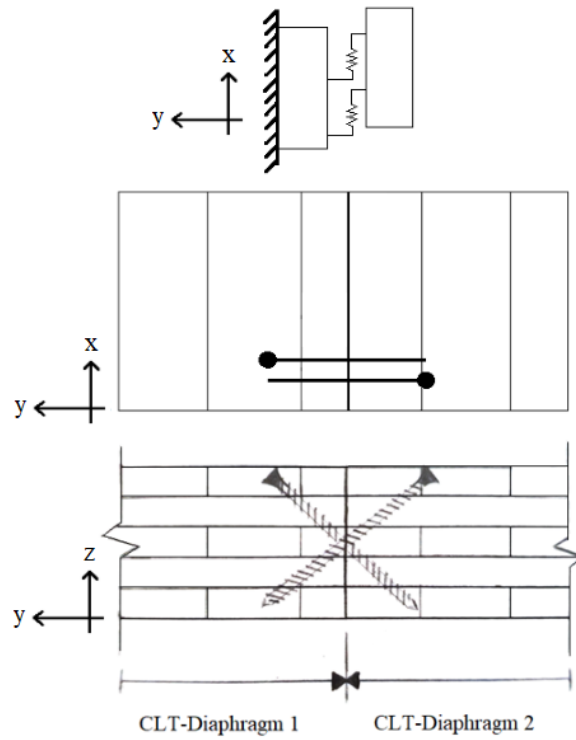


**Figure 3.3:** Illustration of a connection where equation 3.9 is applied with the connection as two springs shown in the top of the connection

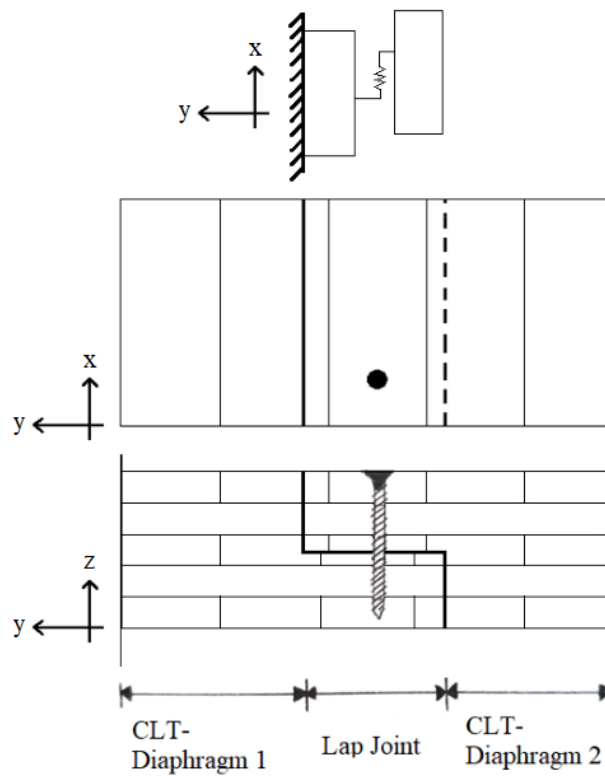


**Figure 3.4:** Illustration of a connection where equation 3.9 is halved with the connection as one spring shown in the top of the connection

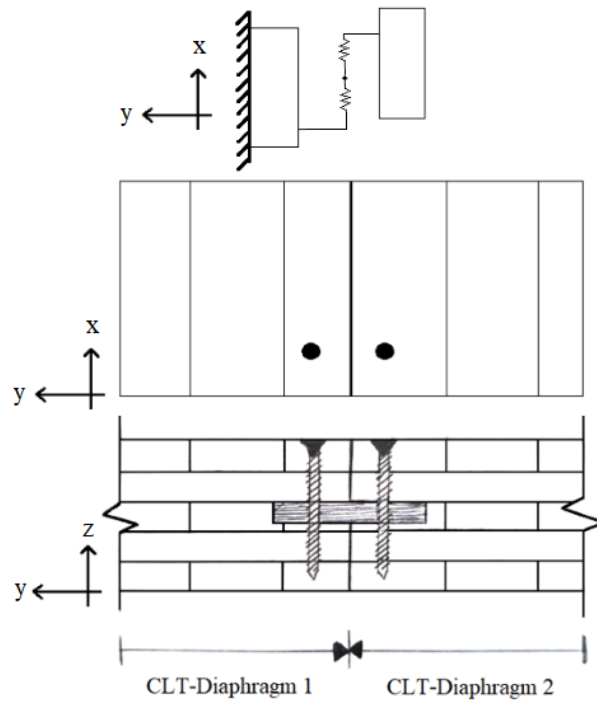


**Figure 3.5:** Illustration of a connection where equation 3.10 is applied with the connection as two springs connected in serie shown in the top of the connection

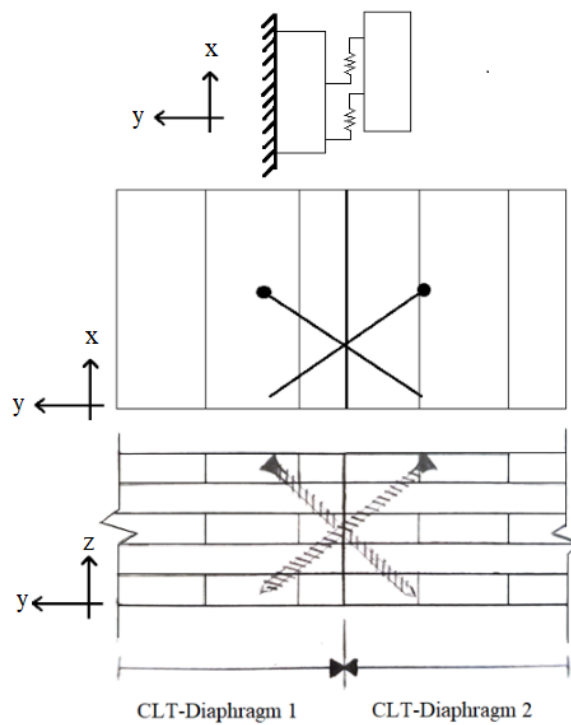


**Figure 3.6:** Illustration of a connection where equation 3.11 is applied with inclined screws with springs shown in the top of the connection

## 3.2 Assumptions for further modeling

### 3.2.1 Diaphragm

Table 3.1 shows the dimensions of the general build-up of the diaphragms used for analytical and numerical calculations with the different parameters presented in figure 3.7. The composition of the model is defined as a 5-layered CLT-diaphragm with an estimation of a common total thickness of 200 mm. The thickness of each board ( $t$ ) is then set as 40 mm and the width of each board is determined as dependent on the thickness of each layer with the width being four times the thickness. The length of the diaphragm was chosen as 6 metres and the width of one CLT panel as 3.0 metres which according to [3] is a commonly applied width. The ratio between diaphragm length and width also allows for square elements being created during FE-mesh in the modeling.

**Table 3.1:** Dimensions of diaphragm

	Value	Unit
Layer thickness, $t$	40	mm
Board width, $b$	160	mm
Diaphragm length, $L$	6000	mm
Diaphragm width, $B$	3000	mm

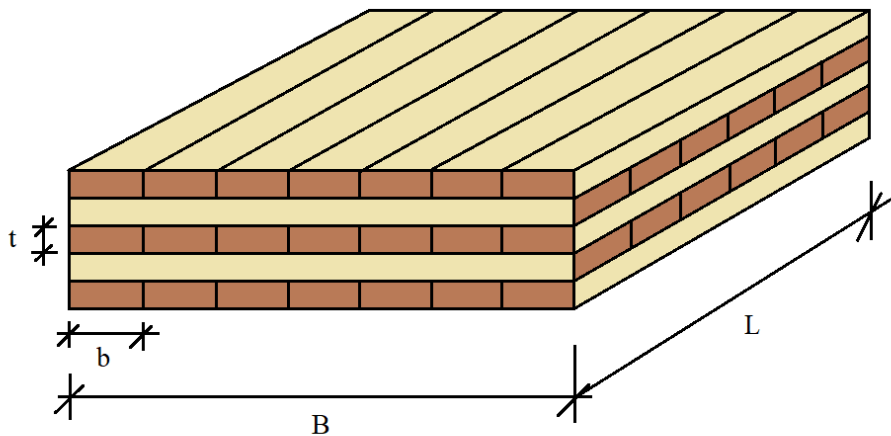


**Figure 3.7:** Illustration of the dimension parameters of a diaphragm

### 3.2.2 Connections

This section presents the configurations of the different connections used in both analytical and numerical modeling. The dimensions of the different screws used in calculations are presented in table 3.2. The inclination of the screws as well as the angle between screw and fibre direction, are presented in table 3.3.

**Table 3.2:** Dimensions of fully threaded self-tapping screws applied

	Shorter screw	Longer screw	Unit
Screw thread diameter, $d$	8	11	mm
Screw inner thread diameter, $d_n$	5	6.6	mm
length of screw, $l$	180	200	mm

**Table 3.3:** Definitions of the angles used for the configuration of the different joints

	Butt joint type 1	Butt joint type 2	Lap joint	Spline connection	Unit
$\alpha$	0	45	0	0	°
$\beta$	30	30	90	90	°
$\gamma$	–	52.2	–	–	°
$\theta$	–	37.8	–	–	°

The configuration of the butt joint connection used for analytical calculations is presented in figure 3.8 with the connection being divided into two types, the first one (type 1) with no angle in the  $xy$ -plane and the other (type 2) with an inclination in the  $xy$ -plane. Both connections are connected with the longer screws. Values used for angles in the model are presented in table 3.3. For the butt joint composition, values of  $\theta$  are simplified assuming either the difference between screw thread and tangential or radial direction of the fibres. The direction of the tangential direction is simplified as 0 degrees and the radial as 45 degrees. Butt joint type 1 is modelled with lateral loaded screw utilizing equation 3.1, equation 3.7 and equation 3.9 since the screws are not loaded by compression and tension forces. Type 2 has screws loaded both laterally and axially and therefore follows all the steps in the section 3.2.3 to determine a relative stiffness for the connection. The value of  $\theta$  for type 2 is chosen for the layer corresponding to the main load-bearing direction as it from calculations will have the largest impact on the effective length of the screws.

The lap joint is illustrated in 3.9 and gives the model applied for analytical calculations together with values for the screw. The screw used for the lap joint is of the shorter version and is installed perpendicular to the  $xy$ -plane without any inclination. The screws are shorter since the screws are not inclined and the thickness of the diaphragm governs the length of the screw in this case. Since the screws are not inclined, equation 3.1 and equation 3.7 are performed before calculating the relative slip modulus. Diaphragms in the lap joint connection are connected with a single screw transferring forces through a connection in a similar manner to a butt-joint connection, but with the exception of only using a single screw in the connection. The result is that equation 3.9 is applied but without doubling the slip modulus.

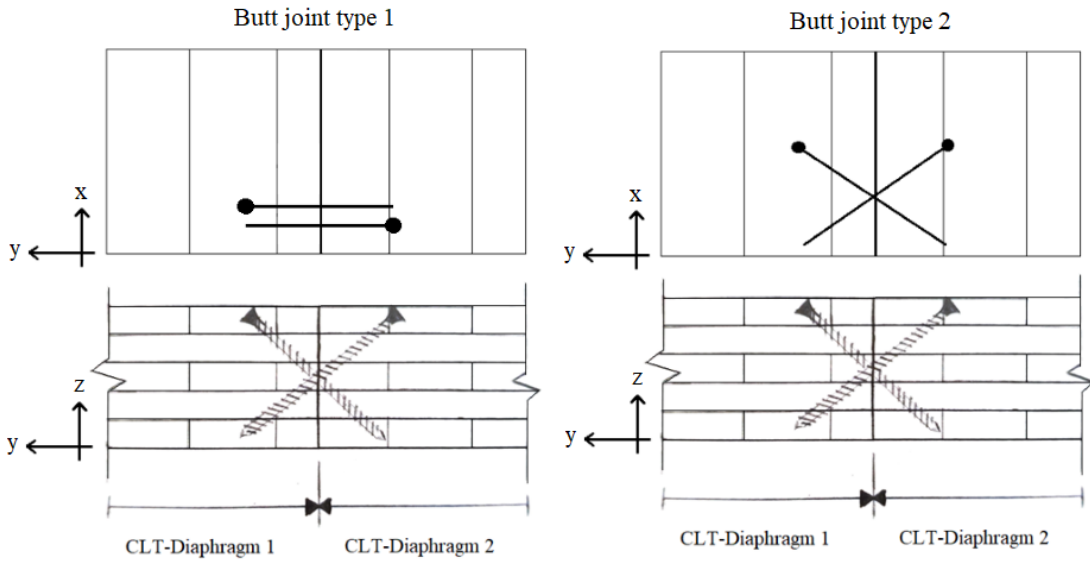


**Figure 3.8:** Illustration of the composition for the two types of butt joints studied

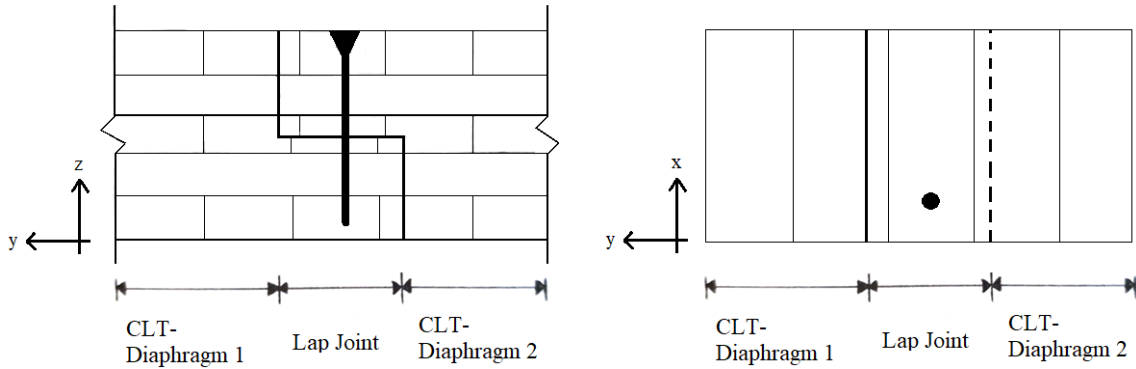


**Figure 3.9:** Illustration of the composition for the Lap joint in modeling

The spline connection applied is done with the same inclination of the screws as the lap joint connection, as seen in table 3.3. The similarity is due to the fact that the screw is not loaded axially. The main difference for calculations are that instead of a single screw, a pair of screws are installed. Figure 3.10 presents the model used for analytical calculations. If one of the screws is removed, forces from one diaphragm can not be transferred to the other. Therefore according to the theory of series connection presented in section 3.1, the final relative elastic stiffness is determined with use of equation 3.10 [6]. Similar to the lap joint connection, equations 3.1 and 3.7 are calculated before any relative elastic stiffness can be defined for the connection.

All the connections are modeled with one screw/pair of screws per metre. The resulting stiffness in the local x-direction, corresponding to the longitudinal direction of the top layer, can be increased by installing multiple screws/pairs of screws per metre along the longitudinal direction of the connected surface.

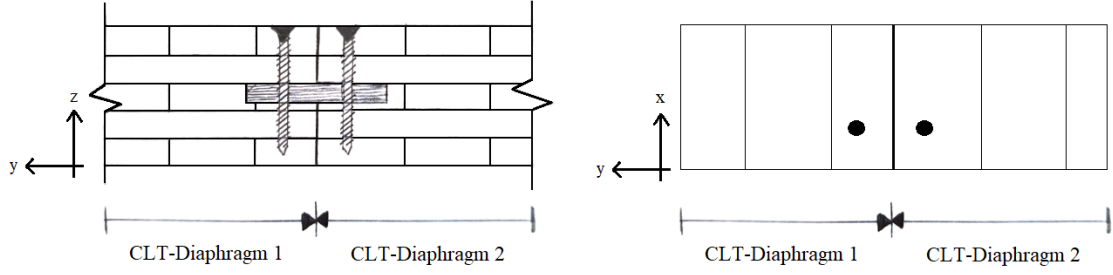


**Figure 3.10:** Illustration of the composition for the Spline connection in modeling

### 3.2.3 Lateral loading

The horizontal loading for calculations is based on the assumption of a rectangular residential building with a flat roof. Both the length and width of the building is assumed to be 21 meters. As expansion in the cities are getting harder due to space limitations, more constructions are built in the suburban area outside of cities. For this project, the building is assumed as a 5-storey, residential building in Hyllie, Malmö. The reference height for the floor segment is set as the fifth storey on a height of 12 meters assuming that each storey including installations is 3 metres high. The basic velocity pressure of wind is determined with a reference wind speed taken from figure 1.4 in [13] and chosen terrain type IV for the imaginable building site. These parameters results in a value of  $0.49 \text{ kN/m}^2$  at a reference height of 12 metres according to table 1.11 in [13]. An exposure factor is determined according to figure 4.2 in [10] which results in a peak velocity pressure presented in equation 3.12.

$$q_p(z) = q_b \cdot c_{e(z)} = q_b \cdot c_{e(12)} = 0.49 \cdot 1.8 = 0.882 \text{ kN/m}^2 \quad (3.12)$$

The external wind pressure coefficient is interpolated for both the windward and leeward side corresponding to the largest factor with values according to [13]. The total wind pressure is the sum of the external wind, both windward and leeward. The largest is chosen as design force shown in equation 3.14. For a floor segment the partial safety factor is chosen as 0.91 for class 2 from table 1.2 in [13]. With a load combination factor of 1.5 for ultimate limit state calculations, the design lateral load used in modeling is given in equation 3.15.

$$Q_k = 0.99 \text{ kN/m}^2 \quad (3.13)$$

$$q_k = Q_k \cdot (1.5 * \text{storeyheight}) = 0.99 \cdot 4.5 = 4.46 \text{ kN/m} \quad (3.14)$$

The multiplication factor for the storeyheight is introduced to consider the wind acting on the top floor and half the wind acting on the storey below.

$$q_d = \gamma_d * 1.5 * q_k = 0.91 \cdot 1.5 \cdot 4.46 = 6.08 \text{ kN/m} \quad (3.15)$$

Determined design value of  $6.08 \text{ kN/m}$  for wind load could be used as input for lateral load in the numerical model to extract results for the project. However, to allow the results to be compared to any lateral load, an arbitrary value of  $1 \text{ kN/m}$  is used. Thereby, the results from this project can be scaled by multiplying the results with a factor corresponding to the different loads.

### 3.3 Numerical modeling for CLT Diaphragms

In this section, the modeling is explained. Support conditions are introduced together with loads before the procedure of extracting results is presented.

#### 3.3.1 Creating the model

To create a model of a floor section, seven panels with length and width according to table 3.1 are inserted into RFEM using rectangular elements. These diaphragms are connected by adjoining the longest sides to each other. The reason for choosing seven panels is based on conversations with supervisors and an estimation of a standard width in multi-storey buildings. The total width of the floor, excluding walls, is 21 metres. Each element is placed next to the previous piece without any distance in between.

#### 3.3.2 Support, hinges and loads

The supports are introduced to manage the movement and rotation for in-plane loading. The model with a simply supported floor resting on two supports loaded with a lateral load is presented in figure 3.11. Initially, two supports are defined for the model as node supports simulating columns. This creates an option to check the forces to the supports, which could be divided as a uniform reaction force on a wall segment as well as a point reaction force on a column. It is assumed for the purpose of modeling that the entire outer line in the longitudinal direction is rigid to avoid any deformations along external walls for the CLT-diaphragm. The exterior lines are introduced as rigid in the member tab during editing of the lines. The variation of force distribution on the supports is analyzed by introducing more nodal supports later on. One outer support is modelled to allow rotation around all axis whilst not allowing displacements in any direction. The other allow rotations in all directions but displacement only in the  $y$ -direction of the model. Two nodal supports with no displacements in the  $z$ -direction are introduced to stabilize the model and these can be seen in the lower corners in figure 3.11. When introducing more supports for analyzing the effects of member and connection stiffness, the added supports are modelled with no displacements in the  $y$ -direction while allowing displacements in  $x$ - and  $z$ -direction as well as rotations around all axes.

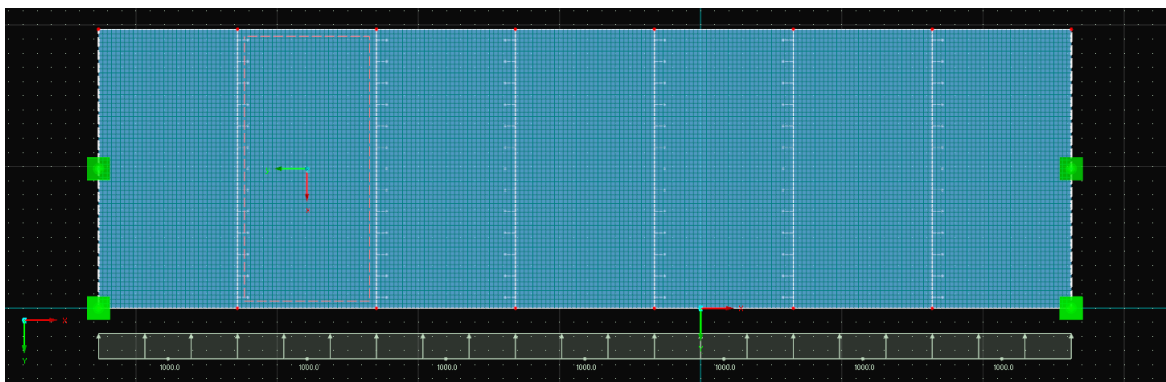


**Figure 3.11:** Illustration of the model as a simply supported floor diaphragm and as seen in RFEM

Hinges are introduced between the rectangular elements as line hinges in the local  $x$ -direction, i.e. along the length of the line. This part is important as this is where the flexibility of the screw connection from the analytical calculations is converted into a spring constant and introduced in the model. An assumption is made that the shear stiffness in the connection acts per metre in both local  $x$ - and  $y$ -axis. The unit is thereby converted from  $N/mm$  to  $N/mm^2$  by dividing the shear stiffness with  $1000\text{ mm}$ . The shear stiffness in the numerical results is coherent with the spring constant  $C_{ux}$  from this point onward. For each analysis the spring constant in the local  $x$ -direction can be altered by changing the value depending on the variable studied. The other spring constants are set as entirely stiff and the same goes for the rotational release in the connection. The hinges are defined the same for all lines in the local  $x$ -direction between two elements.

Lateral loads from wind load are modelled by a uniformly distributed line load with in-plane loading in  $y$ -direction along the shorter side of each element. This creates a load parallel to the connection as seen in figure 3.11. A lateral load of  $1\text{ kN/m}$  is used as input and set as design value.

### 3.3.3 Laminate

After creating the entire model in RFEM, including the supports, the stiffness parameters from the analytical calculation and the loads, the model is converted into a laminate structure. RF-Laminate is an add-on module for RFEM, suitable for CLT since it can define the thickness of layers in an element as well as the orthotropic composition by using an angle rotating the layers according to will [8]. Since the layers in a CLT-diaphragm have different properties depending on the layer, the module is fitted for modeling of a CLT element.

The first part of the Laminate section is to define the surfaces to assign laminate structure. All seven elements in the model are assigned as laminate surfaces. The add-on module also enables the possibility to define material properties which is the following part. First the composition is created for a five-layer CLT element with no edge-glueing and considering coupling in between layers. The composition is presented in table 3.4. This also allows changing the stiffness reduction factors in equation 2.12 which corresponds to equations 2.4 - 2.7 and equation 2.11. After the initial composition, the thickness for each layer is defined together with the orthotropic direction of the layers. Then the modulus of elasticity, shear modulus and Poisson's ratio is chosen for the composition with values presented in table 3.5. The modulus for both MOE and shear is converted from the characteristic values presented earlier into design values by implementing equation 3.16 and equation 3.17. Subsequently, the reference plane is set which for this project is chosen as centered.

$$\begin{aligned}
 E_d &= E_k/\gamma_M \\
 E_{d,x} &= 11000/1.25 = 8800\text{ MPa} \\
 E_{d,y} &= 0\text{ MPa}
 \end{aligned}
 \tag{3.16}$$

$$\begin{aligned}
 G_d &= G_k/\gamma_M \\
 G_{xy} &= G_{xz}690/1.25 = 552\text{ MPa} \\
 G_{yz} &= 50/1.25 = 40\text{ MPa}
 \end{aligned}
 \tag{3.17}$$

**Table 3.4:** Diaphragm composition and orthotropic direction of the layers

	thickness, [mm]	orthotropic direction [°]
layer 1	40	0
layer 2	40	90
layer 3	40	0
layer 4	40	90
layer 5	40	0

**Table 3.5:** Moduli and poisson's ratio inserted into RFEM

	$E_{d,x}$ , [MPa]	$E_{d,y}$ , [MPa]	$G_{xy} = G_{xz}$ , [MPa]	$G_{yz}$ , [MPa]	$\nu_{xy} = \nu_{yx}$ , [-]
layer 1	8800	0	552	40	0

### 3.3.4 Extracting results

The main objective of this project is to study the effects that element- and connection stiffness have on both displacements and reaction force distribution. The procedure of extracting these results is explained below.

#### Convergence

A convergence study is carried out initially to obtain results with a small influence of the element sizes in the FE-mesh. The spring constant for the local  $x$ -axis is set as  $5.4 N/mm^2$  and the reduction factor for element stiffness,  $k_s$  is set as 1.0. The element size for the mesh is varied from 1500 mm to 93.75 mm with each step having half the size of the previous. Maximal displacement is noted for each element size as shown in figure 4.1. The appropriate size used should give a small difference in result compared to previous element size. After some discussion with supervisors, a difference was chosen. When bisecting the element size in the FE-mesh and the difference in displacement between element sizes is between 0.5 and 0.1 % a reasonable size is obtained. A size of 93.75 mm gives a 0.1 % difference in maximal displacement compared to previous size and is used for extracting all further results.

#### Displacements

The displacement is studied for the model with only two outer supports. Initially, the stiffness reduction factor for member stiffness in equation 2.11 is varied while inserting five different values for spring constants in the connections. The spring constant is doubled for each variation of the member stiffness  $k_s$ , with spring constant value starting from  $1 N/mm^2$  and ending at  $16 N/mm^2$ . This will give five different curves and a possibility to study the effect on displacement from element stiffness. The reduction factor is varied from 0.1 to 1.0 with a step of 0.1. Results are for each step extracted by noting the maximal displacement after initializing calculations.

To study the effect on displacement from the shear stiffness, the reduction factor is set as 1.0 while varying the spring constant in the line hinges between 0.5 and 11.5

with a step of 0.5. For each calculation in RFEM the maximal displacement is noted. The effect on displacements in a floor structure from member stiffness and connection stiffness can be analyzed by implementing these steps. An illustrative example of how the floor deforms is presented in figure 3.12.

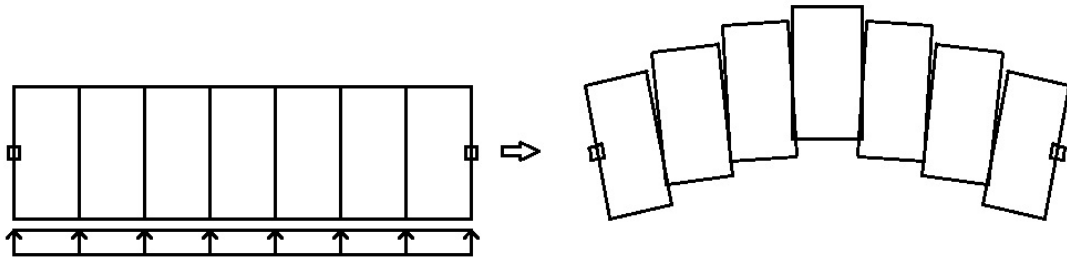


**Figure 3.12:** Illustration of displacement in a floor structure with seven diaphragms due to uniform load

### Reaction forces

Similar to the displacements, the first step is to keep the spring stiffness constant in the line hinges while varying the reduction factor with values according to previous section. Likewise, the second step consists of keeping the reduction factor constant at 1.0 and instead varying the spring stiffness. The difference is the number of supports, changed from 3 to 5 with conditions explained in previous section, for each step. Number of supports are chosen based on the fact that for two supports, the distribution would not change and five supports is assumed as a sufficient maximum amount of supports to study a variation in force distribution. The partition between supports have the same length for each case. For instance, the case with 3 supports have a distance of 10.5 metres between supports. By changing the number of supports and implementing the same steps as for the study of displacements, the variation of reaction force on different supports can be analyzed by again calculating results in RFEM. Results are presented in chapter 5.3.



# 4 Results

In this chapter, the analytical and numerical results from modeling are presented.

## 4.1 Analytical models for shear stiffness in connections

By using equations from chapter 3.1, different values for shear stiffness depending on the type of connection implemented are presented in table 4.1. Values represents the shear stiffness for one screw (lap joint) or pair of screws (butt joint and spline connection) used in the diaphragms per metre. As a result the effectiveness of each connection can be analyzed and discussed in the discussion and conclusion.

**Table 4.1:** Shear stiffness for different types of connection with screws installed once per metre in the local  $x$ -direction (main direction of diaphragm)

Connection	Value	Unit
Butt Joint type 1	5.43	kN/mm
Butt Joint type 2	11.26	kN/mm
Lap Joint	2.06	kN/mm
Spline connection	1.03	kN/mm

As seen in table 4.1, the shear stiffness varies depending on the type of connection applied between diaphragms. Since the calculations are assuming one pair of screws, the value of the shear stiffness depends on the amount of screws used every metre in a connection. Therefore a spline connection with a loose tongue can still be as effective as a butt joint type 2 if more pairs of screws are used per metre.

## 4.2 Numerical modeling for CLT diaphragms

Numerical results presented in this section includes a study of convergence, displacements and force distribution in a floor segment. All results for numerical modeling are plotted in MATLAB using the code given in appendix.

### 4.2.1 Study of convergence

By implementing the procedure explained in chapter 3.3.4 and plotting the results in MATLAB, a convergence can be seen in figure 4.1 which shows a decline in relative difference of the maximum displacement when bisecting the element size.

The plot in figure 4.1 shows that results vary less for smaller element sizes which is reasonable since more elements are considered in the mesh. However, smaller element sizes requires longer computational time to handle the calculations and the amount

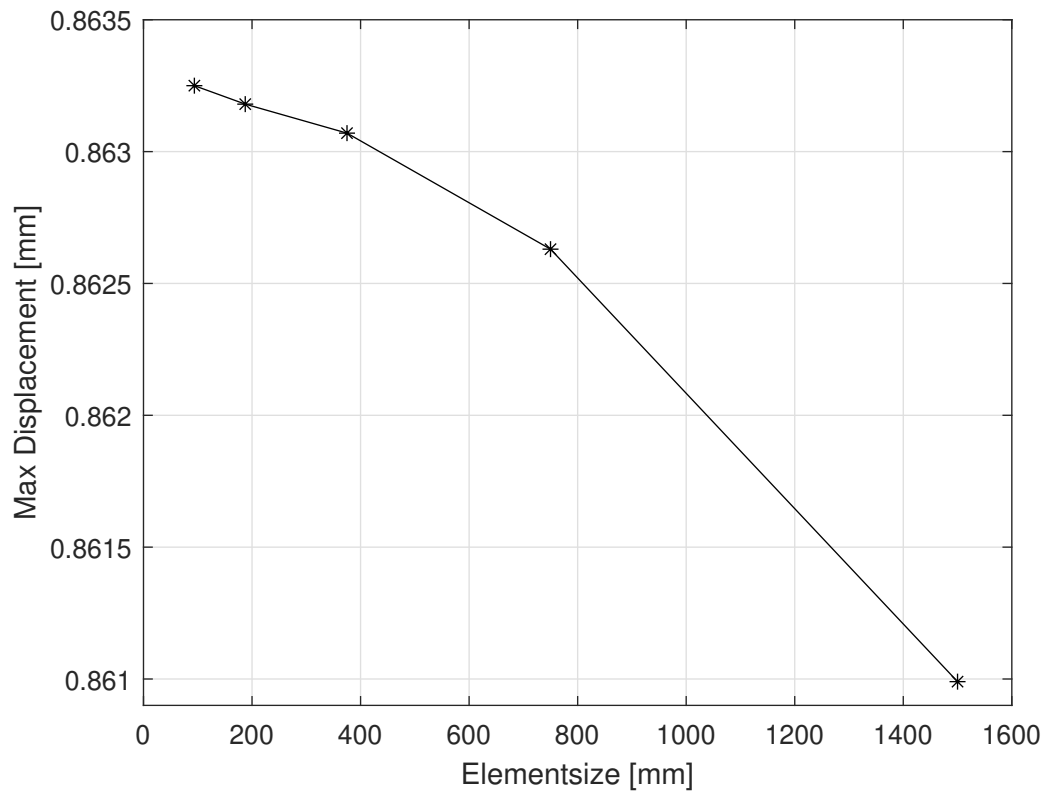


**Figure 4.1:** A study of the results for different mesh-size to achieve correct results for the model

of time needed to process the results increases with declining element size. The time needed to calculate results for a mesh with an element size of  $93.75\text{ mm}$  was low and by bisecting the mesh with a size of  $187.5\text{ mm}$ , the difference in maximal displacement was calculated as  $0.1\%$ . Therefore, this size is assumed to give enough accuracy and reasonable computational time for further calculations. If a more powerful computer had been used with more memory and stronger processor, the results could have been even more accurate.

## 4.2.2 Lateral displacements

This section contains the results of the displacements from modeling in RFEM with displacements being plotted in MATLAB. The model is based on a simply supported beam where maximum lateral displacement being in the middle of the span. An example of how the floor is loaded and the displacement studied is presented in figure 4.2.

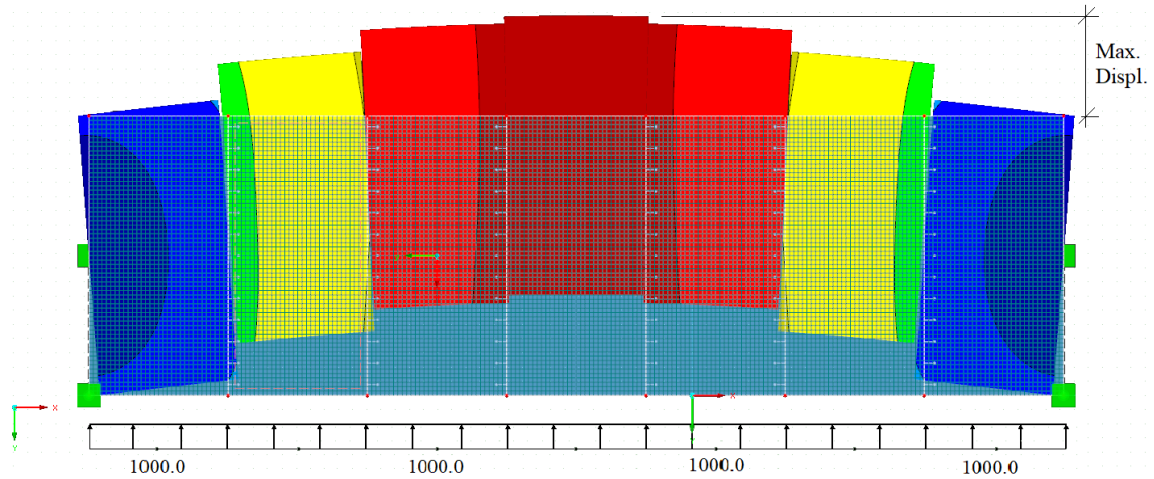


**Figure 4.2:** Lateral displacement due to uniform loading along the width of the floor, as seen in RFEM

### Effect of element stiffness factor

The variation of the reduction factor for CLT panel stiffness,  $k_s$ , results in curves shown in figure 4.3 where the displacement as a function of the reduction factor is illustrated for each of the connection types with spring constants according to table 4.1. Values for displacements correspond to lateral displacement in the global  $y$ -direction. The values for the spring constants are arbitrary values to give an understanding of how the parameter affect the amplitude of the curves in the plot.

A low CLT panel stiffness reduction factor seems to result in a relatively large displacement which follows the theory in section 2.5.1. However, increasing the CLT panel stiffness does not seem to significantly influence the maximum displacement in the span as seen in figure 4.3. When increasing the CLT panel stiffness from a reduction factor of 0.1 to 0.2, the displacement decreases in the structure. However, an increase from  $k_s = 0.2$  to 0.3, the change in displacement is less compared to previous increase of stiffness. The displacements tend not to vary by any significant amount for reduction factors between 0.4 and 1.0. The effect on maximum displacement is similar for all five spring constants studied in the project. With higher stiffness in the CLT panel, the displacements for two higher panel stiffness is presented in table 4.2. Compared to values for no reduction ( $k_s=1.0$ ), an increase in CLT panel stiffness do not decrease the maximum lateral displacement by any significant amount.

For the different curves in figure 4.3, it can be seen that the spring constant in the line hinges affect the amplitude of the curves. Stiffer connections decrease the maximum

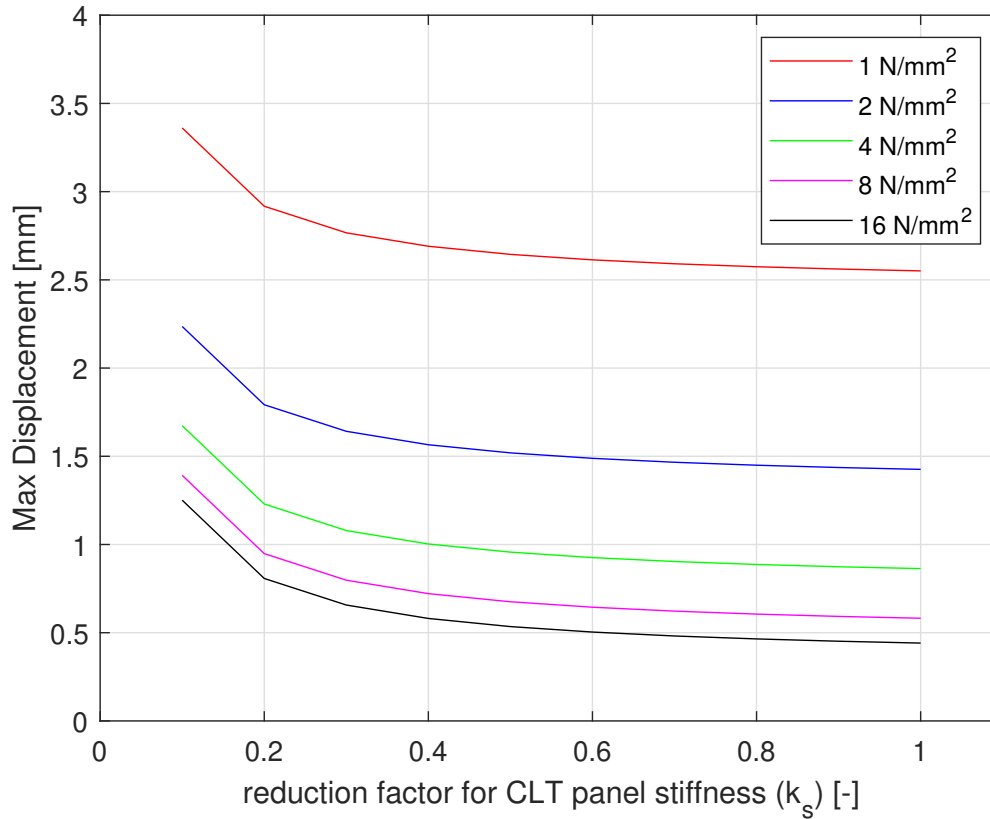


**Figure 4.3:** Lateral displacement as a result of varying the element stiffness reduction factor,  $k_s$  and keeping the spring constant,  $C_{ux}$  in the connection constant for each value shown in figure

displacement when analyzing the effect from diaphragm stiffness but do not effect the inclination of the curve. An increase in connection stiffness seems to follow a non-linear scale, not a linear effect. The difference between a connection with a shear stiffness of 1.0 and 2.0  $N/mm^2$  is 2  $mm$  in figure 4.3. The difference between 2.0 and 4.0  $N/mm^2$  is around 0.6  $mm$  even though the difference in shear stiffness is doubled. Between 4.0 and 8.0  $N/mm^2$ , the difference is around 0.3  $mm$  and when doubling the shear stiffness from 8.0 to 16.0  $N/mm^2$ , the difference is even smaller. A larger shear stiffness in the connection does minimize the lateral displacement in a floor segment but larger values have less impact on the improvement compared to initial increase of shear stiffness.

**Table 4.2:** Maximum displacement [ $mm$ ] for the floor with stiffer CLT panels

	$C_{ux}=1.0$ $N/mm^2$	$C_{ux}=2.0$ $N/mm^2$	$C_{ux}=4.0$ $N/mm^2$	$C_{ux}=8.0$ $N/mm^2$	$C_{ux}=16.0$ $N/mm^2$
$k_s=50$	2.4558	1.3308	0.7683	0.4870	0.3463
$k_s=100$	2.4548	1.3298	0.7672	0.4860	0.3453

### Effect of connection shear stiffness

Figure 4.4 shows the maximal displacement in the simply supported floor structure as a function of varying the spring stiffness in the line hinges. Values for displacements correspond to lateral displacement in the global  $y$ -direction.

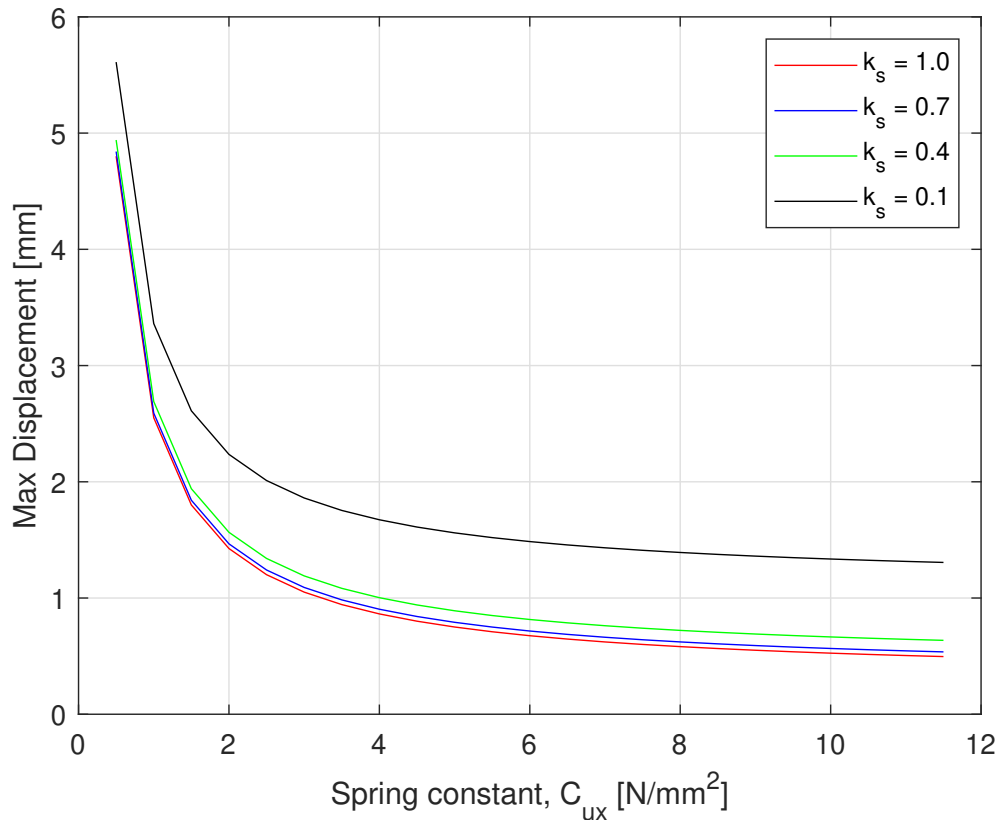


**Figure 4.4:** Lateral displacement as a result of varying the spring constant,  $C_{ux}$  in the connection and keeping the element stiffness reduction factor,  $k_s$  constant at 1.0

Maximum lateral displacement seems to be affected in great length by the shear stiffness in the connection between diaphragms. In comparison with figure 4.3, the curve in figure 4.4 has a steeper inclination for low stiffness values as well as larger displacement in the floor. The curvature declines considerably until reaching a shear stiffness of  $2 \text{ N/mm}^2$ . After reaching  $4 \text{ N/mm}^2$ , the variation is even smaller and can be seen as a sufficient shear stiffness in the connections to minimize the maximum lateral displacement. Higher stiffness do minimize the lateral displacement, but as can be seen in table 4.3, the displacements for higher connection stiffness do not significantly differ from highest shear stiffness in figure 4.3 and figure 4.4.

**Table 4.3:** Maximum displacement [mm] for the floor with stiffer connections

	$k_s=1.0$	$k_s=0.7$	$k_s=0.4$	$k_s=0.1$
$C_{ux}=50 \text{ N/mm}^2$	0.3452	0.3854	0.4846	1.1549
$C_{ux}=100 \text{ N/mm}^2$	0.3223	0.3625	0.4617	1.1320

### 4.2.3 Lateral reaction forces

Reaction forces from RFEM are all divided by the design load of 1 kN/m and the entire width of the floor which results in a factor for the reaction force. The factor is converted into a percentage amount of force distributed on the supports. These steps are presented in equation 4.1. This percentage is compared to factors in [13] which are modified according to equation 4.2. In this project, several interconnected panels are studied, whilst the factors from [13] represents a continuous beam. The reason for illustrating the factor instead of the force from RFEM is to give a general indication of the contributing parameters studied without any specific load. The reason for choosing the evaluated amount of supports is presented in chapter 3.3.4.

$$\text{Factor} = \frac{R_{y,RFEM}}{q_d \cdot 7 \cdot B} = \frac{R_{y,RFEM}}{1 \cdot 21} \cdot \frac{[kN]}{[kN]} = [-] \quad (4.1)$$

$$\text{Amount of force} = J = \text{Factor} \cdot 100 \quad , [\%]$$

$$\text{Amount of force from [13]} = \frac{\text{Factor from [13]} \cdot 100}{n_i} \quad (4.2)$$

$$n_i = \text{number of partitions} = \text{number of supports} - 1$$

When comparing the results of varying the CLT panel stiffness and shear stiffness in the connection, there is a clear difference in the inclination of the curve regardless the number of supports. The shear stiffness in the connection seems almost to have a linear effect on the force distribution, as seen in figure 4.7, 4.10 and 4.13. The CLT panel stiffness factor tends to have a logarithmic growth for the outer supports and logarithmic decay for the middle support, which can be studied in figure 4.6, 4.9 and 4.12.

### Three supports

The model with numbering is presented in figure 4.5. Starting with three supports with a partition length of 11.5 m, figure 4.6 illustrates how the amount of lateral load is distributed on supports as a result of varying the reduction factor,  $k_s$  for the CLT panel stiffness. Figure 4.7 on the other hand, shows the amount of lateral load distributed on supports as a function of varying the shear stiffness in the connection between diaphragms.

The maximum and minimum values for the reaction force from the two parameters are presented in table 4.4 with the shear stiffness having a span of 3.6 times the span of minimum and maximum values for the variation in CLT panel stiffness. Factors in [13] are modified and presented at the bottom of table 4.4.

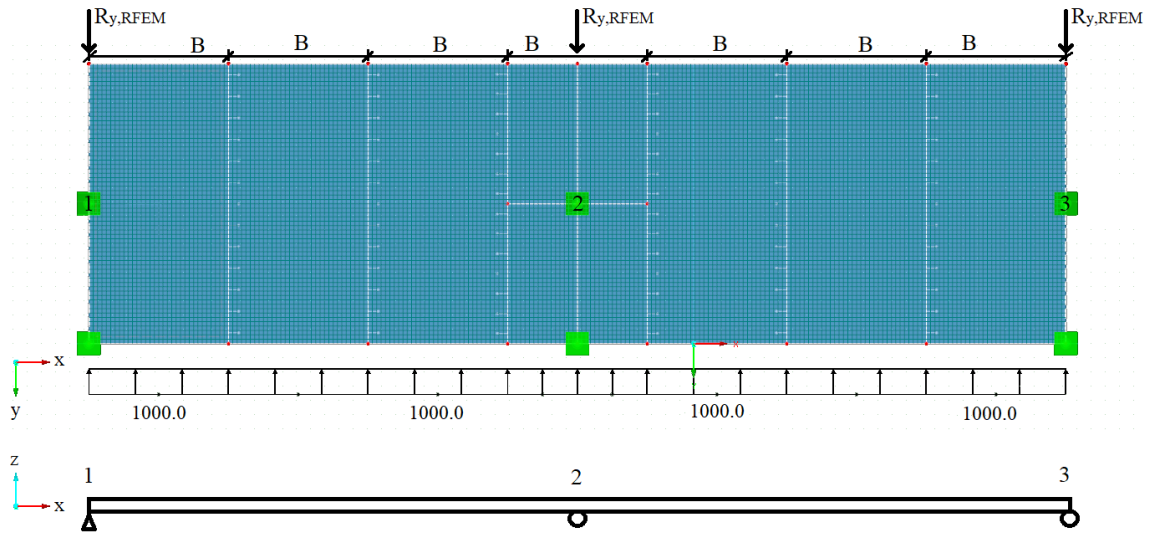


**Figure 4.5:** Illustration of the model with numbering of each support, seen in the  $xy$ -plane (top) and  $xz$ -plane (bottom)

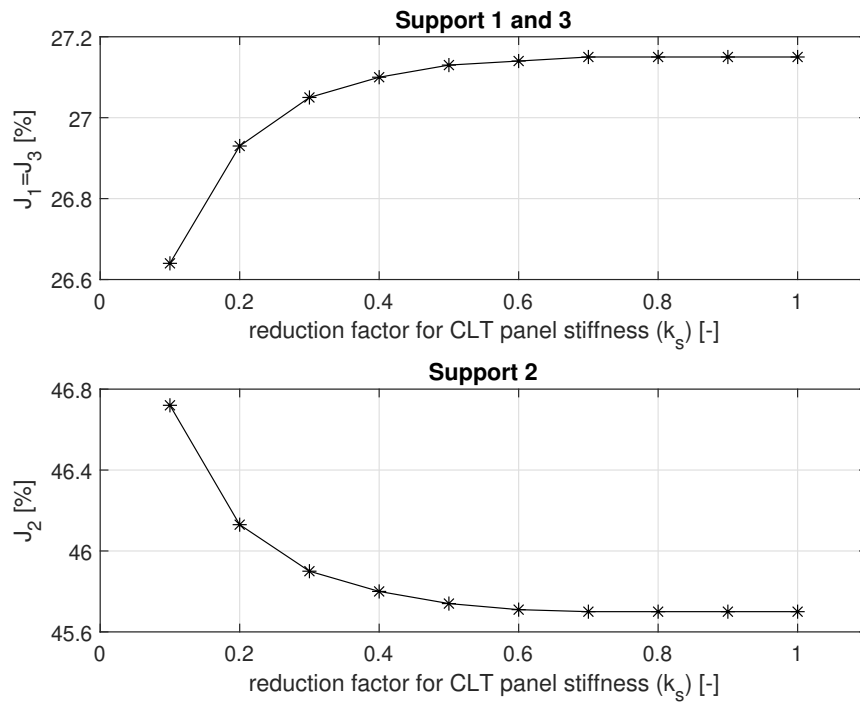


**Figure 4.6:** Amount of force,  $J$  distributed on the supports in case of three supports as a result of varying the element stiffness reduction factor  $k_s$  and keeping the connection spring constant at a constant value of  $4 \text{ N/mm}^2$

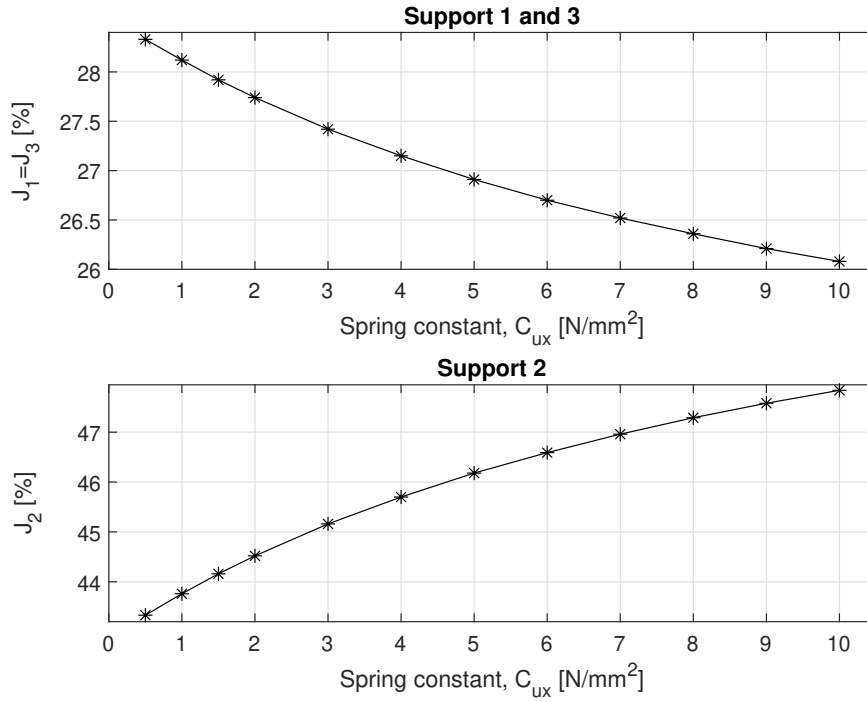


**Figure 4.7:** Amount of force,  $J$  distributed on the supports in case of three supports as a result of varying the spring constant,  $C_{ux}$  in the connection and keeping the element stiffness reduction factor  $k_s$  constant at 1.0

**Table 4.4:** Minimum and maximum amount of force,  $J$  distributed on each support for the model with 3 supports

	$J_1 = J_3$	$J_2$
Minimum value ( $k_s$ varied)	26.6 %	45.7 %
Maximum value ( $k_s$ varied)	27.2 %	46.7 %
Minimum value ( $C_{ux}$ varied)	26.1 %	43.3 %
Maximum value ( $C_{ux}$ varied)	28.3 %	47.8 %
Amount of force according to Euler-Bernoulli beam theory from [13]	18.75 %	62.5 %

## Four supports

Results for the model on four supports are extracted from the model illustrated in figure 4.8 with a partition length of  $5.25\text{ m}$ . By varying the reduction factor,  $k_s$  for the CLT panel stiffness in the model with four supports, the plots in figure 4.9 is obtained. Whereas figure 4.10 illustrates the factor as a function of varying the connection shear stiffness instead of the CLT panel stiffness.

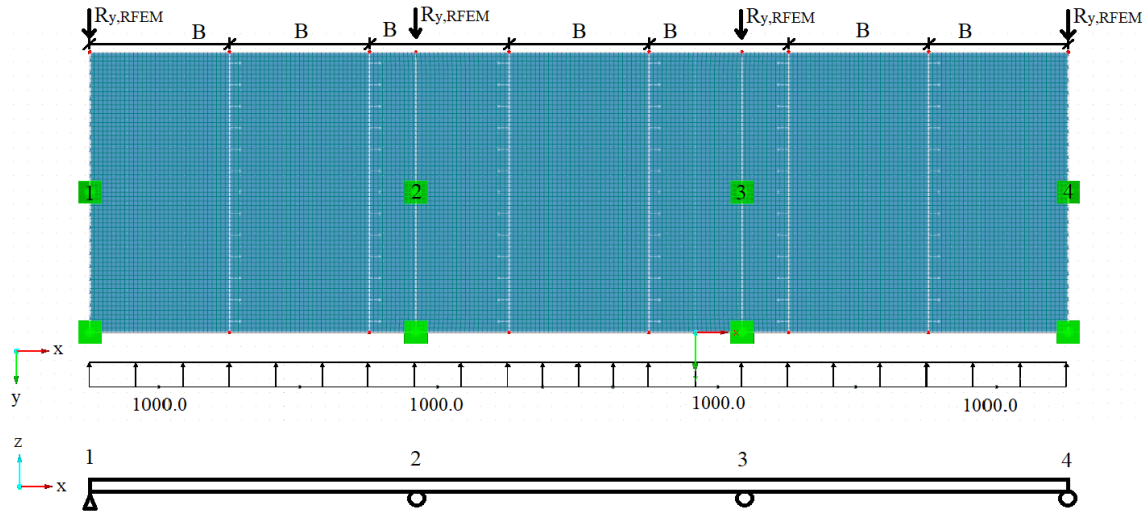


**Figure 4.8:** Illustration of the model with numbering of each support, seen in the  $xy$ -plane (top) and  $xz$ -plane (bottom)

The minimum and maximum amount of force distributed on each support when varying both parameters are presented in table 4.4 with the variation of connection stiffness resulting in a larger difference between minimum and maximum force distribution. A homogeneous beam supported on four supports with the same length but, with a constant bending stiffness along the length as well as the thickness gives factors in [13], which are modified and presented at the bottom of table 4.5.

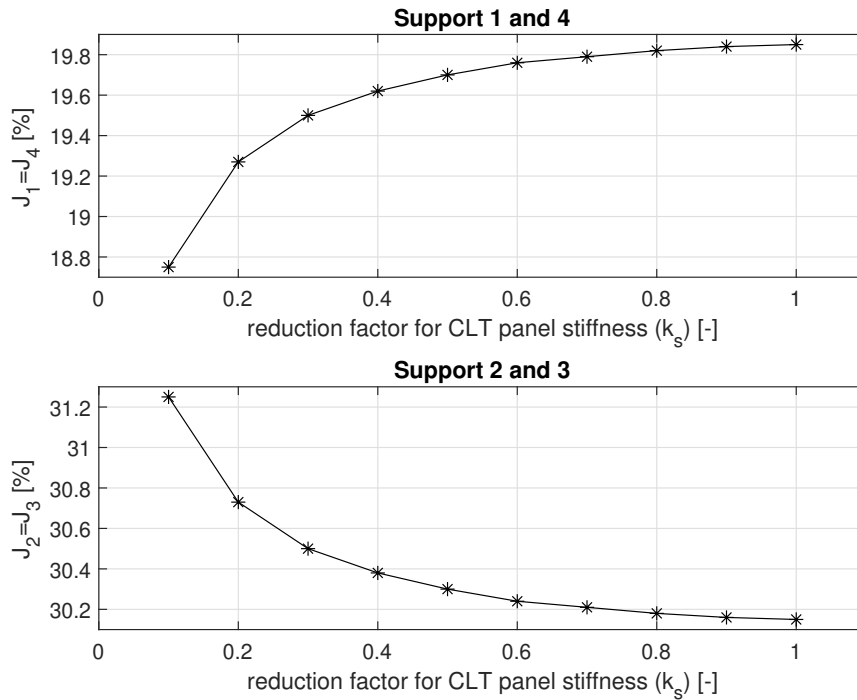


**Figure 4.9:** Amount of force,  $J$  distributed on the supports in case of four supports as a result of varying the element stiffness reduction factor  $k_s$  and keeping the connection spring constant at a constant value of  $4 \text{ N/mm}^2$

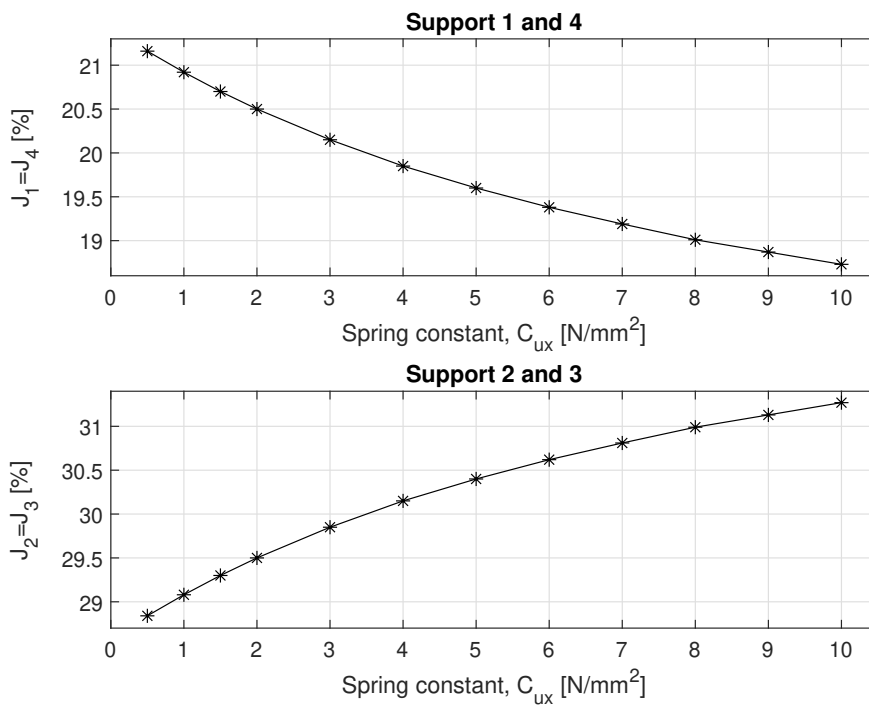


**Figure 4.10:** Amount of force,  $J$  distributed on the supports in case of four supports as a result of varying the spring constant,  $C_{ux}$  in the connection and keeping the element stiffness reduction factor  $k_s$  constant at 1.0

**Table 4.5:** Minimum and maximum amount of force,  $J$  distributed on each support for the model with 4 supports

	$J_1 = J_4$	$J_2 = J_3$
Minimum value ( $k_s$ varied)	18.8 %	30.1 %
Maximum value ( $k_s$ varied)	19.9 %	31.3 %
Minimum value ( $C_{ux}$ varied)	18.7 %	28.8 %
Maximum value ( $C_{ux}$ varied)	21.2 %	31.3 %
Amount of force according to Euler-Bernoulli beam theory from [13]	13.3 %	36.7 %

### Five supports

The model with five supports is loaded and supported as illustrated in figure 4.11 with the numbering of each support included together with the CLT panel width and the reaction force. Figure 4.12 and figure 4.13 illustrates how the distribution of reaction forces changes depending on the variation of CLT panel stiffness respectively shear stiffness in the connection. Since the model is symmetric the figures only shows three supports even though there are actually five supports. The outer supports have the same distribution and the same goes for the second and fourth support in the model.

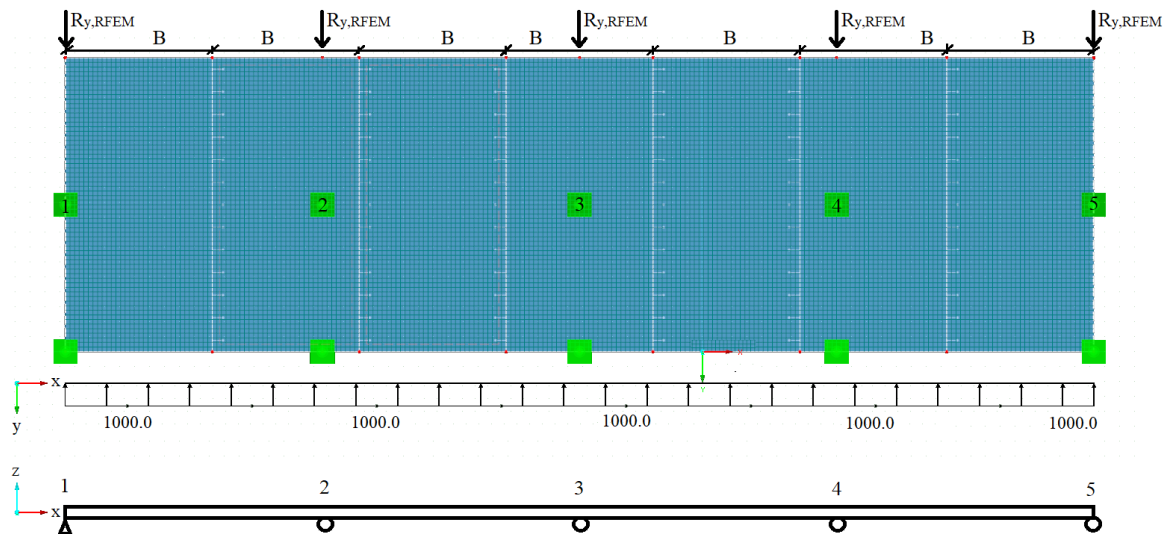


**Figure 4.11:** Illustration of the model with numbering of each support, seen in the  $xy$ -plane (top) and  $xz$ -plane (bottom)

Minimum and maximum amount of force,  $J$  on each support is presented in 4.6 for both the parameters. The amount of force distributed on each support can be compared to factors for a homogeneous beam with five supports and a uniformly distributed load where the stiffness is constant along both longitudinal direction and along the thickness of the panel. Those values are taken from [13] and have a distribution presented in the end of table 4.6.

In the case of five supports along the width of the floor, the curve inclination is the same as in the case with three and four supports. The main difference is that for  $J_3$  have a similar curvature as  $J_1$  and  $J_5$ . However, the force distributed to the middle support do not increase as fast as for the outer supports due to a larger portion of the reaction force being distributed to the outer supports. Also, For  $J_3$  there is a difference where the difference between the minimum and maximum force is affected more by the CLT panel stiffness than the shear stiffness. For  $J_2$  and  $J_4$ , the difference in minimum and maximum amount of force when varying the CLT panel stiffness parameter is the same as when varying the shear stiffness.  $J_1$  and  $J_2$  have a larger difference when the connection stiffness is varied.

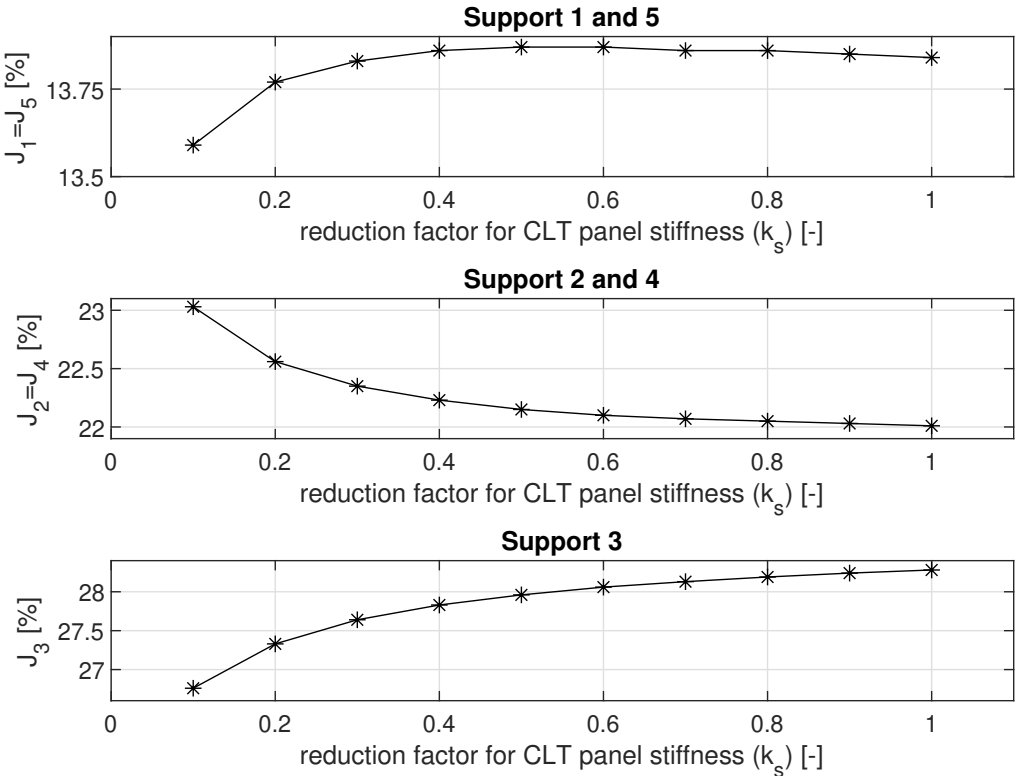


**Figure 4.12:** Amount of force,  $J$  distributed on the supports in case of five supports as a result of varying the element stiffness reduction factor  $k_s$  and keeping the connection spring constant at a constant value of  $4 \text{ N/mm}^2$

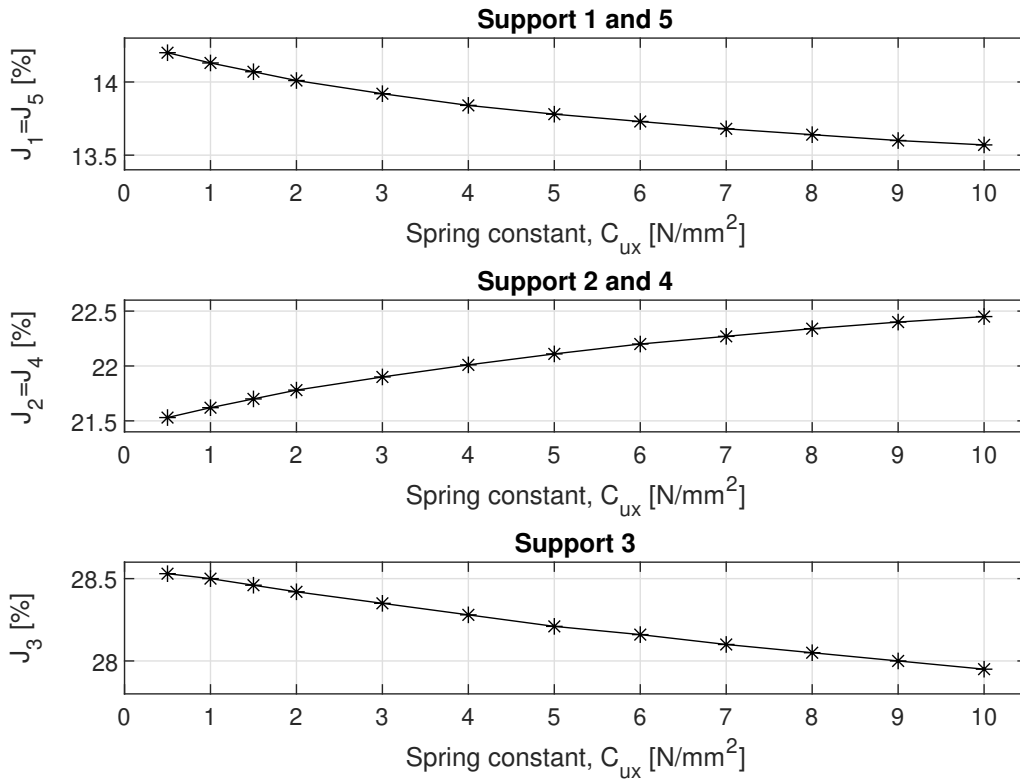


**Figure 4.13:** Amount of force,  $J$  distributed on the supports in case of five supports as a result of varying the spring constant,  $C_{ux}$  in the connection and keeping the element stiffness reduction factor  $k_s$  constant at 1.0

**Table 4.6:** Minimum and maximum amount of force,  $J$  distributed on each support for the model with 5 supports

	$J_1 = J_5$	$J_2 = J_4$	$J_3$
Minimum value ( $k_s$ varied)	13.6 %	22.0 %	26.8 %
Maximum value ( $k_s$ varied)	13.8 %	23.0 %	28.3 %
Minimum value ( $C_{ux}$ varied)	13.6 %	21.5 %	28.0 %
Maximum value ( $C_{ux}$ varied)	14.2 %	22.5 %	28.5 %
Amount of force according to Euler-Bernoulli beam theory from [13]	9.8 %	28.6 %	23.2 %



# 5 Discussion

Results from both analytical and numerical calculations are, in this chapter, discussed to analyze possible improvements to achieve better results. A general discussion regarding the connection of elements is included in the first part of the discussion. At the end of this chapter, the challenges concerning the project are analyzed and discussed.

## 5.1 General discussion

Both practical installation, production implementation and economical aspects are important when choosing a connection for CLT-diaphragms. From a production point of view, the easiest would be the butt joint solution for joining CLT-diaphragms. But, the practical installation on site would probably prefer a lap joint or a spline connection which doesn't require as much accuracy when inserting the screws. However, from an economical point of view, the less screws used per metre can minimize costs even if only a little. Then there is also the question of wasted wood when joining CLT-elements to consider. One can argue for the strength of each type of connection from a certain point of view. From the literature review done, there seems to be missing a suggested interval for displacements in the horizontal direction. Therefore, the conclusions made for displacements in this project can't be compared to any standards and give an indication of the accuracy of the results. The lateral load for numerical modeling is based on an arbitrary load. Wind load calculated could have been used, but since the load differs from the number of storeys as well as the geographical position, an arbitrary load of  $1 \text{ kN/m}$  is applied instead. However, the calculated wind load gives a perspective of the magnitude in lateral load which acts on the assumed building and therefore, the displacements and reaction forces in the model can still be interpreted by scaling the results.

## 5.2 Analytical results

Most analytical calculations made are based on Eurocode which lacks potential influencing parameters. In the equations for slip modulus, the diameter of the screws, effective length and the density of the diaphragm are used. It does not matter which screws are used considering the strength. For a spline connection, a possible parameter could be the material used for the spline. A piece of plywood instead of steel would probably have an impact on the stiffness in the connection. Another parameter which is studied is the inclination of the screws in the connections which, for the butt joint, has a large impact on the shear stiffness. The inclination helps transfer both compression and tension forces which makes the connection more sturdy. Lap joints consist of one screw and therefore the combination of both handling tension and compression is not possible for inclined screws. The literature review regarding spline connections never mentioned the use of inclination of screws which possibly could be implemented for such connections and as seen in the results, impact the shear displacements and force distribution of spline connections. It is important to understand that the results from the analytical models are based on a certain combination in diameter and length as

well as type of screw. A partially threaded self tapping screw would have different values compared with the fully threaded used in analytical models. Self-tapping screws are easy to install but possibly not the only used in reality and therefore results can vary depending on initial values used as input.

### 5.3 FE-model

The results regarding force distribution to the different supports, values for percentage of force distributed to the supports seem to point towards a realistic result. Diaphragms are divided into several elements connected in between and allowing movement due to not being completely rigid. Therefore, the amount of force in numerical modeling are necessarily not the same as the factors from [13].

The model includes line hinges instead of point hinges. It would be possible to introduce pairs of screws at certain points to analyze if the distribution of load to supports would differ. Since the supports are modelled with a point support, the support would be a pillar, not a wall. A wall segment would instead divide the point load along the line. However, to resemble such supports, the edges along the global  $y$ -direction are modelled as rigid and therefore remaining straight when deforming which can be seen in figure 4.2. As for the case of reaction force distribution, the model could be improved to introduce uneven spans to accommodate the possibility to design the interior for different sizeable apartments with different distances in the interior of the building. Such a case would certainly change the distribution but would no longer be comparable to the factors from [13].

Regarding displacement, the largest displacement from numerical calculations was determined as 3.4  $mm$  when varying the element stiffness and 5.6  $mm$  when varying the shear stiffness in the connections. These values are determined for a lateral load of 1  $kN/m$ . From the analytical calculations, a wind load of 6.08  $kN/m$  would have larger deflections, with values around six times higher than values from the numerical modeling. An increase of lateral displacement would probably not change the inclination of the curve. The results could therefore still be interpreted as what parameter affect the deflection the most and what value for shear stiffness is recommended to have a small variation in increased deflection. The shear stiffness in the connection seems to affect the displacement in a floor more than the actual stiffness in the diaphragm. A less stiff floor with a sufficient stiffness in between diaphragms will still more or less act as a whole diaphragm. On the contrary, a floor with no reduction of the CLT panel stiffness but less stiffness in between panels will act as several diaphragms and result in greater lateral displacements. This follows the theory of a series connection in mechanics from [6], with the diaphragms seen as series connected. When minimizing the stiffness between elements, the diaphragms are subjected more as individual elements by lateral forces instead of acting as a unit.

The lateral force distribution on supports seems to be affected by low CLT panel stiffness in a greater way compared with the shear stiffness in the connections due to the initial steeper inclination of the curves. However, the difference in the amount of force,  $J$  distributed to each support is more considerable when varying the shear stiffness for all supports. Another interesting difference between both paramet-

ers is that the increase in amount of force,  $J$  distributed on supports is opposite for the two. An increase in CLT panel stiffness augments the amount of reaction force in the outer support whereas an increase of shear stiffness between diaphragms decreases the amount of force distributed on the outer support. The amount of reaction force distributed to the middle support decreases when stiffening the element but increases when adding more shear stiffness in the connections. An increase in shear stiffness between element tends to distribute the forces towards the theoretical factors from [13] as a result of acting as one unit instead of seven panels. This could be an explanation of why the shear stiffness results in such a distribution when stiffening the connections. Another reason for why the factors differs is the theory of how they are determined. Theoretical factors from [13] follows the Euler-Bernoulli beam theory where as the results from modelling follows the Timoshenko beam theory. The Timoshenko beam theory accounts for shear forces contrary to Euler-Bernoulli theory and therefore it is not difficult to understand that the lateral force distribution would differ between the two theories. Regarding the floor, with an increase in CLT panel stiffness, the reaction forces in the outer supports increase. It could be possible due to the fact that the outer supports can carry more of the load not being dependent on the shear stiffness in the connections to transfer loads to the middle support. This could explain the results when analyzing the variation of CLT panel stiffness.

The difference of the amount of force presented in table 4.4, 4.5 and 4.6 indicates how much focus needs to be placed on each parameter to determine that the supports are designed for a certain amount of distributed lateral loading. What can be seen as the main difference when adding supports is that the force is distributed in the floor more evenly and that the CLT panel stiffness has an increased influence on the reaction forces.

## 5.4 Challenges in the project

One initial challenge of the project was defining the area of work which initially focused on the shear stiffness of the connection. As the project progressed, the reduction factor for the diaphragm itself became a major part of the entire project .

Another factor still important to discuss is the guidelines for lateral displacements in floor. Today, in EC, there is recommendations for vertical deflections in SLS but not for lateral displacements. Mainly, when people spend time in a building, they tend to react to a floor with large deformations in a vertical direction as well as vibrations in the floor. Lateral movement could be felt in the same way especially as a sign of earthquakes. For the reason of the lack of guidelines, it would be preferable to compare values from the results to some guidelines to see what stiffness is required in both the diaphragms and in the connections between.

Further challenges included modeling the floor system as a realistic floor structure. The walls were swapped for pillars when analyzing the force distribution to the supports. The lateral loading was the only load acting on the building as both external and internal vertical loads were neglected. The line hinges in the connections were only defined in the model as spring constants in the longitudinal direction, not in the transverse direction. The floor section did not include any cuts for stairs etc. which could have affected the behaviour of the structure due to the floor not being symmetrical anymore. Both aspects studied, deformation and force distribution, would probably have varied more than the results given above.

Finally, one challenge was concerning how to compare the analytical and numerical results in a correct way without changing the input too much. To give an indication of the results, the comparison must be similar, otherwise the conclusions made could be misleading. More parameters would complicate and too few would not give a proper answer. The time is of course another challenge as limitations of the work is needed to handle the time-frame. A more complete structure in the model would be preferable but that includes more work and also the possibility to miss certain important effects which would lead to a more complex situation to analyze.

# 6 Conclusion

## 6.1 Project conclusions

From analytical calculations, it is clear that the Butt joint connection exhibits the highest shear stiffness compared to both the the Lap joint and Spline connection with a loose tongue. Especially the second composition of Butt joint with inclined screws taking forces in tension/compression as well as shear, indicates a higher shear stiffness. The main difference is the angle of the screws and according to what theory the screws are connected. It is clear that a series connection is less stiff compared to a connection with diaphragms connected according to theory of parallel connections (top in figure 3.3). If both screws take up forces from the same diaphragm, one screw will still transfer forces even if the other one fails. Further, the inclination of the screws contributes to increased stiffness of the connection through handling shear forces as well as compression and tension forces flowing in the connection. To obtain the same stiffness in the connection as in a Butt joint type 2, more screws can be installed with ease. The practical difference between the stiffer type of connection and the other two is that its harder to install as it requires precision when installing the screws at a certain angle.

The displacement is affected to a greater extent by the shear stiffness in the connection as lower stiffness results in an exponentially increasing lateral displacement. However, for both the element stiffness and the shear stiffness in the connection, there seems to be a limit for when the displacement does not increase much. For the variation in element stiffness, a reduction factor between 0.3 and 1.0 will not vary the displacement in a considerable way. For the connections, a shear stiffness of  $4 \text{ N/mm}^2$  will suffice to ensure that the diaphragms does not deform in lateral direction by any substantial number. Higher stiffness can be used to increase the overall stiffness of the diaphragm, but the effect would not be as big as when increasing from lower values to  $4 \text{ kN/mm}$ . More screws also means more use of material and the needed increase of steel material can in a larger picture have a negative effect on the climate.

Regarding the force distribution from lateral loads on supports, it is clear that more supports have a positive effect on the structure as the load is divided on more supports. In the case of five supports with an even span between, most of the horizontal load will go to the middle support and the least of the load will go to the outer supports. This is valid for both the variation of element stiffness as well as for the variation of shear stiffness in the connection. For the most evenly distributed force distribution for all supports, the focus should be on the shear stiffness in the diaphragm as the factors for the different supports have a smaller difference compared to the impact from element stiffness. However, if the building has multiple walls or pillars that do not carry as much load, a few crucial walls and pillars can be used. In that case, the element stiffness should be in focus. When adding more supports, the difference between maximum and minimum values tends to increase which is why the two parameters are important to consider to ensure the right dimensions on supports. By dividing a homogeneous beam into multiple diaphragms and keeping the number of supports the same, the reaction forces seems to distribute more evenly across the floor. Diaphragms with a

stiffness reduced by no more than 0.5 combined with a shear stiffness of  $5 \text{ N/mm}^2$  will create a relatively even distribution.

## 6.2 Future work

This project only focuses on supports handling lateral forces. Since there is need to handle vertical forces from snow load, dead load etc. as well as horizontal loads, a continuation of this study could be to analyze the effects from both horizontal and vertical load for other suitable types of connections.

Another parameter could be to do physical tests of the connections evaluated in this project to give a practical indication of how the results from modeling in a software according to theoretical calculations match reality. The model and theoretical calculations does not necessarily take into account the human errors, imperfections in the material due to knots, moisture or bending of the lamels. A laboratory testing of the connections and diaphragms is recommended to support the results calculated in this project.

A concluding remark of a continuation of this project is to evaluate and produce some guidelines for acceptable displacements in the horizontal direction due to lateral loads which are missing in EC today.

# Bibliography

- [1] M. Augustin, J. Koppelhuber, K. Pock and M. Wallner-Novak. *Cross-Laminated Timber Structural Design II - Applications*. proHolz Austria, 2018. ISBN: 978-3-902320-96-4.
- [2] E. Borgström. *Design of timber structures - Structural aspects of timber construction*. Swedish Wood, 2016.
- [3] E. Borgström and J. Fröbel. *CLT Handbook, CLT structures - facts and planning*. Stockholm: Swedish Wood, 2019.
- [4] R. Brandner, G. Flatscher, A. Ringhofer, G. Schickhofer and A. Thiel. *Cross laminated timber (CLT): overview and development*. Vol. 74. 3. 2016, pp. 331–351.
- [5] D.M. Carradine. *Methodology for the Design of Timber Frame Structures Utilizing Diaphragm Action*. 2002.
- [6] O. Dahlblom, S. Heyden, A. Olsson and A. Sandberg. *Introduktion till strukturmekaniken*. Studentlitteratur, 2008. ISBN: 9789144051253.
- [7] Deutsches Institut für Bautechnik. *European Technical Approval ETA-11/0190 - Würth self-tapping screws for use in timber constructions*. 2013, pp. 1–62.
- [8] Dlubal Software GmbH. *Add-on Module - RF-LAMINATE - Design of Laminate Surfaces - Program Description*. 2016, pp. 1–97.
- [9] M. Dördüncü. *Coupling of Peridynamics and Timoshenko Beam Theory for the Stress Analysis of Laminated Composite Materials*. Vol. 14. 1. 2021, pp. 53–62.
- [10] European Committee for Standardization, EN 1991-1-4. *Eurocode 1:Actions on structures - Part 1-4: General actions - Wind actions*. Swedish Standards Institute, 2005.
- [11] European Committee for Standardization, EN 1995-1-1. *Eurokod 5:Dimensionering av träkonstruktioner - Del 1-1:Allmänt - Gemensamma regler och regler för byggnader*. Swedish Standards Institute, 2009.
- [12] J. Fröbel. *Design of timber structures - Rules and formulas according to Eurocode 5 and EKS 9 (BFS 2013:10) including material properties*. Swedish Wood, 2019.
- [13] A. Isaksson T. Mårtensson. *Byggnadskonstruktion, Regel- och formelsamling, Upplaga 3:1*. Studentlitteratur, 2017.
- [14] R. Jockwer, R. Steiger and A. Frangi. *Design model for inclined screws under varying load to grain angles. Proceedings of the 1st Meeting of the International Network on Timber Engineering Research (INTER 2014)*. Timber Scientific Publishing, KIT Holzbau und Baukonstruktionen, 2014.
- [15] C. Loss, A. Hossain and T. Tannert. *Simple cross-laminated timber shear connections with spatially arranged screws*. Vol. 173. Elsevier Ltd., 2018, pp. 340–356.

- [16] I. Lukacs, A. Björnfort and R. Tomasi. *Strength and stiffness of cross-laminated timber (CLT) shear walls: State-of-the-art of analytical approaches*. Vol. 178. 2019, pp. 136–147.
- [17] Mass Timber Connections (MTC). *CLT Connections Design Guide*. Mass Timber Connections, 2019.
- [18] Naturvårdsverket. *Bygg- och fastighetssektorns klimatpåverkan*. 2020. URL: <https://www.naturvardsverket.se/Sa-mar-miljon/Klimat-och-luft/Klimat/Tre-satt-att-berakna-klimatpaverkande-utslapp/Bygg--och-fastighetssektorns-klimatpaverkan/>.
- [19] N. Ottosen and H. Petersson. *Introduction to the Finite Element Method*. Prentice Hall Europe, 1992. ISBN: 978-0-13-473877-2.
- [20] Swedish Wood. *Stabiliserande system - generellt*. 2003. URL: <https://www.traguiden.se/konstruktion/konstruktiv-utformning/stomme/stomme/stabiliserande-system/>.
- [21] Swedish Wood. *Stabiliseringssystem för flervåningshus*. 3. 2018. URL: <https://www.svensktra.se/publikationer-start/tidningen-tra/2018-3/stabiliseringssystem-for-flervaningshus/>.
- [22] Swedish Wood. *Properties of softwood*. n.d. URL: <https://www.swedishwood.com/wood-facts/about-wood/from-log-to-plank/properties-of-softwood/>.
- [23] M Wallner-Novak, J Koppelhuber and K Pock. *Cross-laminated timber structural design—basic design and engineering principles according to Eurocode*. 2014.
- [24] S. Zoellig, M. Muster and A. Themessl. *Butt-joint bonding of timber as a key technology for point-supported, biaxial load bearing flat slabs made of cross-laminated timber*. 323rd ed. Vol. 323. 2019, p. 012144.

# Bilaga A

## Appendix

The MATLAB code used for plotting of all results is written below.

```
function Exjobbsresultat
```

Convergence, studying the effect from FE-mesh size on deflections with  $k_s = 1.0$  and  $C_{ux} = 4.0 \text{ N/mm}^2$

```
figure(1)
x = [1500750375187.593.75];
y = [0.860990.862630.863070.863180.86325];
plot(x,y,'-k*')
xlim([0 1600])
ylim([0.86090 0.8635])
grid on
xlabel('Elementsize [mm]')
ylabel('Max Displacement [mm]')
```

Study of lateral deformations as a result of varying the diaphragm's stiffness whilst keeping the shear stiffness in the connections constant at 4 kN/mm

```
Defkserx = linspace(0.1,1.0,10);
y1 = [3.3609 2.9173 2.7666 2.6905 2.6444 2.6134 2.5912 2.5744 2.5613 2.5508];
figure(2)
plot(Defkserx,y1,'-r')
hold on
y2 = [2.2358 1.7921 1.6416 1.5654 1.5193 1.4884 1.4661 1.4494 1.4363 1.4258];
plot(Defkserx,y2,'-b')
hold on
y3 = [1.6733 1.2295 1.0790 1.0029 0.9568 0.9258 0.9036 0.8868 0.8738 0.8633];
plot(Defkserx,y3,'-g')
hold on
y4 = [1.3919 0.9482 0.7977 0.7215 0.6754 0.6445 0.6223 0.6055 0.5924 0.5819];
plot(Defkserx,y4,'-m')
hold on
y5 = [1.2511 0.8074 0.6569 0.5808 0.5347 0.5037 0.4815 0.4648 0.4517 0.4412];
plot(Defkserx,y5,'-k')
legend('1 N/mm2', '2 N/mm2', '4 N/mm2', '8 N/mm2', '16 N/mm2')
xlabel('reduction factor for CLT panel stiffness ( $k_s$ ) [-]')
ylabel('Max Displacement [mm]')
xlim([0 1.1])
ylim([0 4])
grid on
```

hold off

Study of lateral deformations as a result of varying the shear stiffness in the connections whilst not reducing the diaphragm's stiffness

```
Defksx = linspace(0.5,11.5,23);
figure(3)
y1 = [4.8008 2.5508 1.8008 1.4258 1.2008 1.0508 0.9436 0.8633 0.8007 0.7507 0.7098
0.6757 0.6469 0.6221 0.6007 0.5819 0.5654 0.5507 0.5375 0.5257 0.5149 0.5052 0.4963];
plot(Defksx,y1,'r')
hold on
y2 = [4.8412 2.5912 1.8412 1.4661 1.2411 1.0911 0.9840 0.9036 0.8411 0.7911 0.7502
0.7161 0.6872 0.6625 0.6410 0.6223 0.6057 0.5910 0.5778 0.5660 0.5553 0.5455 0.5366];
plot(Defksx,y2,'b')
hold on
y3 = [4.9405 2.6905 1.9404 1.5654 1.3404 1.1904 1.0833 1.0029 0.9404 0.8904 0.8494
0.8153 0.7865 0.7617 0.7403 0.7215 0.7050 0.6903 0.6771 0.6652 0.6545 0.6448 0.6359];
plot(Defksx,y3,'g')
hold on
y4 = [5.6109 3.3609 2.6108 2.2358 2.0108 1.8608 1.7536 1.6733 1.6107 1.5607 1.5198
1.4857 1.4568 1.4321 1.4106 1.3919 1.3753 1.3606 1.3474 1.3356 1.3249 1.3151 1.3062];
plot(Defksx,y4,'k')
legend('ks = 1.0', 'ks = 0.7', 'ks = 0.4', 'ks = 0.1')
xlabel('Spring constant, Cux [N/mm2]')
ylabel('Max Displacement [mm]')
grid on
```

Force distribution depending on amount of supports and the diaphragm's stiffness whilst keeping the spring constant in the connections,  $C_{ux} = 4 \text{ N/mm}^2$

```
Lastkserx = linspace(0.1,1.0,10);
```

3 supports

```
R1=[26.64 26.93 27.05 27.10 27.13 27.14 27.15 27.15 27.15 27.15];
R2=[46.72 46.13 45.90 45.80 45.74 45.71 45.70 45.70 45.70 45.70];
figure(4)
subplot(2,1,1)
plot>Lastkserx,R1,'-k*')
title('Support 1 and 3')
xlabel('reduction factor for CLT panel stiffness (ks) [-]')
ylabel('J1=J3 [%]')
xlim([0 1.1])
ylim([26.6 27.2])
grid on
subplot(2,1,2)
plot>Lastkserx,R2,'-k*')
title('Support 2')
xlabel('reduction factor for CLT panel stiffness (ks) [-]')
ylabel('J2 [%]')
```

```

xlim([0 1.1])
ylim([45.6 46.8])
grid on

4 supports
R1=[18.75 19.27 19.50 19.62 19.70 19.76 19.79 19.82 19.84 19.85];
R2=[31.25 30.73 30.50 30.38 30.30 30.24 30.21 30.18 30.16 30.15];
figure(5)
subplot(2,1,1)
plot(Lastkserx,R1,'-k*')
title('Support 1 and 4')
xlabel('reduction factor for CLT panel stiffness ( $k_s$ ) [-]')
ylabel('J1=J4 [%]')
xlim([0 1.1])
ylim([18.7 19.9])
grid on
subplot(2,1,2)
plot(Lastkserx,R2,'-k*')
title('Support 2 and 3')
xlabel('reduction factor for CLT panel stiffness ( $k_s$ ) [-]')
ylabel('J2=J3 [%]')
xlim([0 1.1])
ylim([30.1 31.3])
grid on

5 supports
R1=[13.59 13.77 13.83 13.86 13.87 13.87 13.86 13.86 13.85 13.84];
R2=[23.03 22.56 22.35 22.23 22.15 22.10 22.07 22.05 22.03 22.01];
R3=[26.76 27.33 27.64 27.83 27.96 28.06 28.13 28.19 28.24 28.28];
figure(6)
subplot(3,1,1)
plot(Lastkserx,R1,'-k*')
title('Support 1 and 5')
xlabel('reduction factor for CLT panel stiffness ( $k_s$ ) [-]')
ylabel('J1=J5 [%]')
xlim([0 1.1])
ylim([13.5 13.9])
grid on
subplot(3,1,2)
plot(Lastkserx,R2,'-k*')
title('Support 2 and 4')
xlabel('reduction factor for CLT panel stiffness ( $k_s$ ) [-]')
ylabel('J2=J4 [%]')
xlim([0 1.1])
ylim([21.9 23.1])
grid on
subplot(3,1,3)
plot(Lastkserx,R3,'-k*')

```

```

title('Support 3')
xlabel('reduction factor for CLT panel stiffness ( $k_s$ ) [-]') ylabel('J3 [%]')
xlim([0 1.1])
ylim([26.6 28.4])
grid on

```

Force distribution depending on amount of supports and the shear stiffness in the connections while diaphragm's stiffness is not reduced,  $k_s = 1.0$

```

Lastk88=[0.5 1 1.5 2 3 4 5 6 7 8 9 10];
3 supports
R1=[0.2833 0.2812 0.2792 0.2774 0.2742 0.2715 0.2691 0.2670 0.2652 0.2636 0.2621
0.2608]*100;
R2=[0.4333 0.4376 0.4416 0.4452 0.4516 0.4570 0.4618 0.4659 0.4696 0.4729 0.4758
0.4784]*100;
figure(7)
subplot(2,1,1)
plot(Lastk88,R1,'-k*')
title('Support 1 and 3')
xlabel('Spring constant, Cux [N/mm2]')
ylabel('J1=J3 [%]')
xlim([0 10.5])
ylim([26.0 28.4])
grid on
subplot(2,1,2)
plot(Lastk88,R2,'-k*')
title('Support 2')
xlabel('Spring constant, Cux [N/mm2]')
ylabel('J2 [%]')
xlim([0 10.5])
ylim([43.2 47.95])
grid on

```

```

4 supports
R1=[0.2116 0.2092 0.2070 0.2050 0.2015 0.1985 0.1960 0.1938 0.1919 0.1901 0.1887
0.1873]*100;
R2=[0.2884 0.2908 0.2930 0.2950 0.2985 0.3015 0.3040 0.3062 0.3081 0.3099 0.3113
0.3127]*100;
figure(8)
subplot(2,1,1)
plot(Lastk88,R1,'-k*')
title('Support 1 and 4')
xlabel('Spring constant, Cux [N/mm2]')
ylabel('J1=J4 [%]')
xlim([0 10.5])
ylim([18.6 21.3])
grid on
subplot(2,1,2)

```

```

plot(Lastk88,R2,'-k*')
title('Support 2 and 3')
xlabel('Spring constant,  $C_{ux}$  [ $N/mm^2$ ]')
ylabel('J2=J3 [%]')
xlim([0 10.5])
ylim([28.7 31.4])
grid on

```

5 supports

```

R1=[0.1420 0.1413 0.1407 0.1401 0.1392 0.1384 0.1378 0.1373 0.1368 0.1364 0.1360
0.1357]*100;

```

```

R2=[0.2153 0.2162 0.2170 0.2178 0.2190 0.2201 0.2211 0.2220 0.2227 0.2234 0.2240
0.2245]*100;

```

```

R3=[0.2853 0.2850 0.2846 0.2842 0.2835 0.2828 0.2821 0.2816 0.2810 0.2805 0.2800
0.2795]*100;

```

```

figure(9)

```

```

subplot(3,1,1)

```

```

plot(Lastk88,R1,'-k*')

```

```

title('Support 1 and 5')

```

```

xlabel('Spring constant,  $C_{ux}$  [ $N/mm^2$ ]')

```

```

ylabel('J1=J5 [%]')

```

```

xlim([0 10.5])

```

```

ylim([13.4 14.3])

```

```

grid on

```

```

subplot(3,1,2)

```

```

plot(Lastk88,R2,'-k*')

```

```

title('Support 2 and 4')

```

```

xlabel('Spring constant,  $C_{ux}$  [ $N/mm^2$ ]')

```

```

ylabel('J2=J4 [%]')

```

```

xlim([0 10.5])

```

```

ylim([21.4 22.6])

```

```

grid on

```

```

subplot(3,1,3)

```

```

plot(Lastk88,R3,'-k*')

```

```

title('Support 3')

```

```

xlabel('Spring constant,  $C_{ux}$  [ $N/mm^2$ ]')

```

```

ylabel('J3 [%]')

```

```

xlim([0 10.5])

```

```

ylim([27.8 28.6])

```

```

grid on

```